# Final Report

# RAYLEIGH WAVES

by Eduard Berg



May 1976



Sponsored by Advanced Research Projects Agency
ARPA Order 1827





APPROVED: George P. Woollard
G. P. Woollard, Director
Hawaii Institute of Geophysics

Program Code: 4F10
Grantee: University of Hawaii, Hawaii Institute of Geophysics
Effective Date: 1 Oct. 1973
Expiration Date: 31 March 1976
Amount of Grant: $57,739

Grant No.: AFOSR-74-2612
Principal Investigators:
E. Berg, ph. 808-948-8762
G.H. Sutton, ph. 808-948-8761
Program Manager:
Mr. William J. Best AFOSR
ph. 202-693-0162

Outline

# ABSTRACT

For a signal-to-noise ratio between 0.2 and 0.1 on the original single-component records, amplitudes for Rayleigh waves over oceanic paths of 155° at station MAT and 98° at station KIP have been determined as 12 mμ and 24 mμ peak-to-peak, respectively, with a standard error of less than 11 per cent. In each case the processed correlation signal is the highest in a half-hour record. The method makes use of preliminary high-pass filtering and normalized reference earthquake-matched filtering, and takes full advantage of the well-dispersed oceanic surface wave.

The method also provides high resolution of co-located events with short time separation, or of widely spaced events with Rayleigh waves arriving nearly simultaneously at a single station, when the summed vertical and radial matched filtered components are used. Examples include: (1) clear separation and amplitude determination at stations KIP and MAT of two $M_s$ = 6.5 earthquakes located 0.7° and 145 sec apart off the coast of central Chile; (2) clear separation at station KIP of a Novaya Zemlya $m_b$ = 4.8 event from interfering Rayleigh waves of an $m_b$ = 5.0 Kermadec Island earthquake arriving 120 to 140 sec prior to the searched event, with almost complete elimination of interference on the summed vertical and radial processed components; and (3) clear separation at station KIP of two co-located $m_b$ = 4.4 and 4.5 earthquakes 6 min apart off the coast of Chile, with determination of their amplitudes in the presence of interfering Rayleigh waves from two central Alaska earthquakes, the first ($m_b$ = 4.1) arriving 15 min prior to the first Chile Rayleigh wave and the second between the two Chile arrivals.

The single-station threshold reached (10 and 25 digital units, p-p) for stations MAT and KIP at 155° and 98°, respectively, corresponds to an $M_s$ = 3.3 and probably can be improved further. Beam focusing is obtained by referring the individual station correlation (reference earthquake matched filter) outputs to the origin time and summing these output from the array of the randomly spaced HGLP stations.

It is shown that the computer determined magnitudes (relative to the reference event) are very stable among different components and different stations and varying by less than 0.1 magnitude.

Automated amplitude and phase response of the complete seismometer-recording system is obtained from step inputs to the calibration coil. High accuracy is achieved by summing as many pulses as desired (to eliminate background noise) by a correlation technique and subsequent Fourier analysis. The only parameters required are the seismometer mass, the Cal-coil constant (referred to the center of mass if appropriate) and current, and the precise onset time of one reference calibration current, which are all very stable over long time periods. Application to the High Gain Long Period system at KIP yields the magnification curve from only six pulses with less scatter ($< \pm 5\%$ for periods larger than 20 sec) than routine steady-state calibrations.

Deconvolution of the digital seismograms results in retrieval of the ground motion (in the frequency range of interest) by the use of the complex Fourier coefficients obtained from the calibration method.

All computer programs developed or used for purpose of this work are presented in a (separate) report.

# I Introduction

A number of carefully designed, 3-component High Gain Long Period (HGLP) seismometer stations have been installed in several locations. This network is aimed at exploring the worldwide, stable earth-noise background window between 30 and 40 sec period and lowering the threshold of detectable surface waves. Gains from ground motion to record trace amplitude for "good" stations (OGD and CTA) are typically over 100,000 in the frequency band of the noise window, whereas those stations located in areas of high oceanic microseism (like KIP) have magnifications from 20,000 to 40,000. Many of these HGLP stations are located in and around the Pacific.

The reported noise background of the better stations (15 to 25 mμ at 40 sec period) is such that earthquakes with $M_s(T=40) = 2.1$ should be detected at a distance of 25°, those with $M_s(T=40) = 3.1$ near 90°. This is based on the 40 sec surface wave magnitude determination using Gutenberg's attenuation as $\Delta^{-1.66}$ ($\Delta$ = distance in degrees) beyond $\Delta = 25°$ and assuming that signal-to-noise ratio on the record is near 1:1 for visual detection of the surface waves by a trained observer. The magnitude of detectable earthquakes will be up to 0.4 higher for the HGLP stations with the lesser gains.

In the original proposal the Pacific HGLP stations were considered as a randomly spaced array and we had suggested a combination of beam steering and signal extraction methods in the presence of high, but uncorrelated noise, in order to lower the detection threshold for small-magnitude shallow-focus earthquake around the Pacific. It was further suggested to study the variation of Rayleigh wave radiation pattern for different periods and for the same source areas, and investigate attenuation of 40 sec Rayleigh waves across the Pacific.

This study was aimed at testing regional focal mechanism stability of shallow focus earthquakes of small magnitudes so that reference signals at a given station in the $m_B$ range from 5 to 5.5 could be used for extracting signals of earthquakes of smaller magnitudes by cross-correlation methods that are more promising when the signals are well dispersed. Oceanic Rayleigh wave signals are well dispersed for periods shorter than 25 to 28 sec (Oliver, 1962; Kuo et al., 1962) especially when the generally long travel path from circum-Pacific earthquake waves to the KIP station are considered. The cross correlation, in addition, when normalized to the reference event signal will yield the magnitude for the small quake and can be based on a selected frequency band.

Other methods succeeding in signal-to-noise ratio improvements, such as polarization filtering of Love and Rayleigh waves (Simmons, 1968; Choy and McCamy, 1973) were not considered at this point.

The regionalization approach avoids the uncertainties involving the distortion of the Rayleigh waves spectrum due to frequency, path and station site dependence, since only events from the same source area at a given station are compared, a point recently stressed by Alexander (1973)

Preliminary visual inspection of the high gain photographic records from KIP for the first one-half to two-thirds of each of the months of September, October and November 1973 indicated that many closely matched Rayleigh wave trains could be found that would be suitable for digital processing. These included earthquakes from off the coast of Chile, off the coast of Mexico,

Gulf of Mexico, Gulf of Alaska, Kurile Island area, Luzon-Philippine, Fiji, south of Kermadec and the mid-Atlantic ridge. Preliminary locations were obtained from LASA/Norsar bulletins. An example of matching signals from the Fiji area is shown in Fig. 1 for $m_B$ (LASA) from 3.9 to 4.5.

As a result a digital tape and computer plotted records for selected events were obtained from the Albuquerque Seismological Center (ASC), aimed primarily at the use for establishing and verifying the computer programs. For further check on matching of Rayleigh waves, earthquakes from the south of Kermadec area (on October 15, 1973; $m_B$ from 5.1 to 3.7) had been included, only the larger shock was given in the LASA bulletin. The smaller shocks could be identified by their almost perfect match of surface waves over 10 to 15 minutes. The time difference of occurrence was determined from this match (± 1 sec) and later confirmed from the NOAA/USGS PDE cards. Use of Everden's

$$M_s = \log \frac{A}{T} + 1.00 \log \Delta + 0.92$$

yields $M_s(38) = 4.4$ for the largest and $M_s = 3.6$ for the smallest shock. Gutenberg's formula results in a 0.2 higher magnitude. It was therefore anticipated that shocks of $M_s = 3.0$ to 3.3 could be identified for this area in the normal background noise of the KIP station. Similarly Kurile Island earthquakes near 45.8N and 151.7E could be recognized down to $M_B = 4.3$ (4 October 1973 origin time G.S. 185701.6, $M_B = 4.3$, normal depth, p-p amplitude on record 3mm ($M_s$ (calculated from $M_B$) = 2.9) at a distance near 5200 km). However, comparing the p-p amplitude

to the 3 October 1974 quake (p-p amplitude on photographic record 84 mm) yields a $M_s$ of 3.1.

Figure 3 shows the (signal + noise)/noise power density (smoothed over 5 data points) for the Kurile Island earthquake. The vertical component had instrument correction included and is the same as in Fig. 2 whereas the horizontal component did not include instrumental corrections. Signal to noise power exceeds 300. Assuming signal to noise power near 1 for detection the threshold magnitude would be 1.24 lower than the one for this 3 October 1973 Kurile Island earthquake or near 3.3 ($M_s$) which is in good agreement with visual results of the preceding section.

No cross-correlation methods had been used so far but an improvement of between 0.3 to 0.5 in $M_s$ of the threshold was expected.

The power spectra also suggested a prefiltering to eliminate noise at periods (longer than 40 to 50 sec.) where essentially no useful signal was found.

## References to Introduction

Alexander, S. S.: Final Report, Long-Period Seismic methods for identifying small, underground Nuclear Explosions, the Pennsylvania State University, Dept. of Geosciences, 151 pages, 1973.

Choy, George and Keith McCamy: Enhancement of Long-Period Signals by Time-Varying Adaptive Filters, Journal of Geophysics Research; Vol. 78, No. 17, pp. 3505-3511, June 1973.

Kuo, John, James Brune and Maurice Major: Rayleigh Wave Dispersion in the Pacific Ocean for the Period Range 20 to 140 seconds, Bulletin of the Seismological Society of America, Vol. 52, No. 2, pp. 333-357, April 1962.

Oliver, Jack, A Summary of Observed Seismic Surface Wave Dispersion, Bulletin of the Seismological Society of America, Vol. 52, no. 1, pp. 81-86, January 1962.

Savino, John, Keith McCamy and George Hade: Structures in Earth Noise Beyond Twenty Seconds - A Window for Earthquakes, Bulletin of the Seismological Society of America, Vol. 62, No. 1, pp. 141-176, Feb. 1972.

Simons, R.S.: A Surface wave Particle Motion Discrimination Process, Bulletin of the Seismological Society of America, Vol. 58, No. 2, pp. 629-637, April 1968.

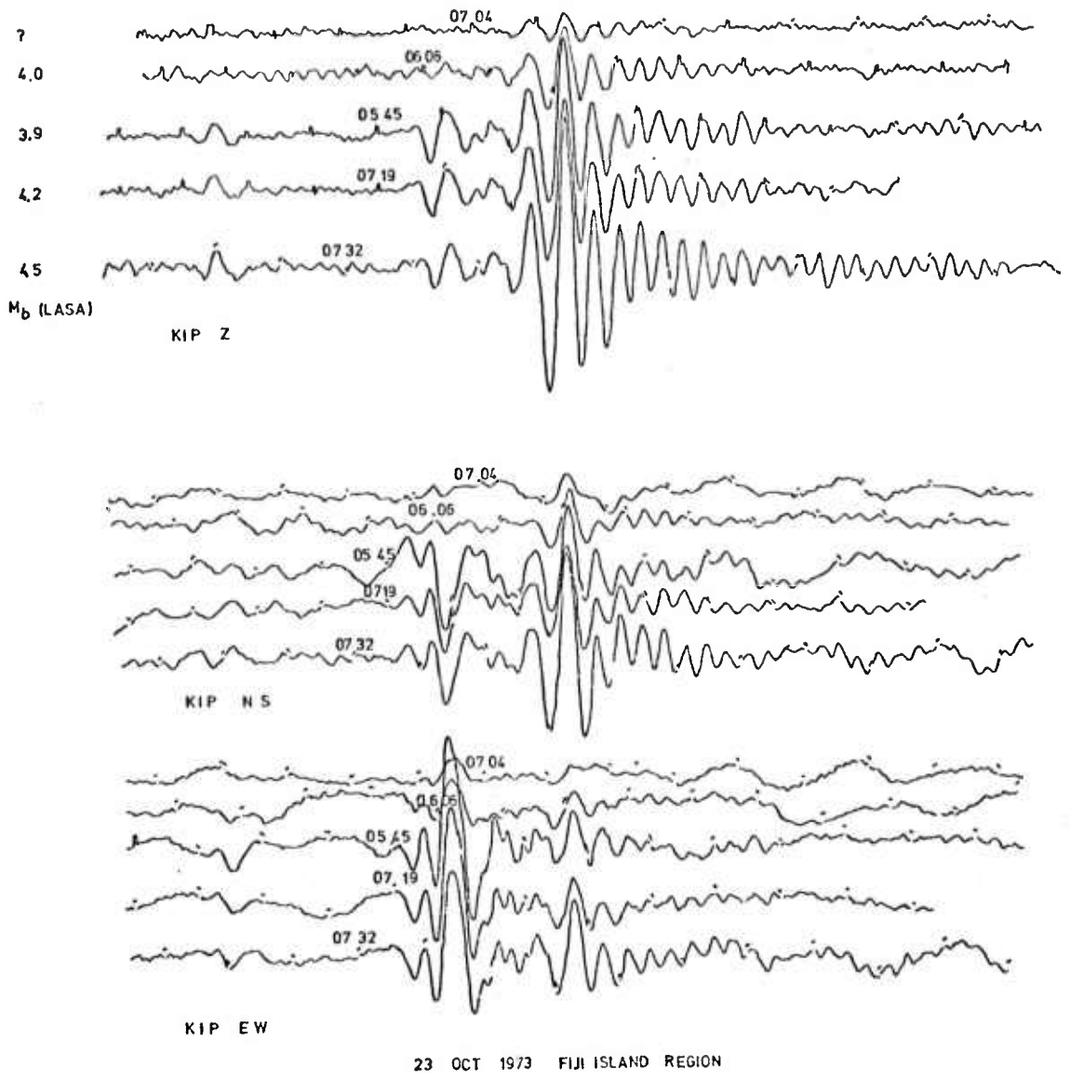


Fiji Island earthqaukes redrawn from photographic records. Nearly identical signals indicate constant focal mechanism. None were listed in either the NORSAR bulletin or the U.S.G.S. monthly listings. Four are given by the LASA bulletin. The smallest one ( not listed ) has a surface wave magnitude of 3.2 .

Fig. 1

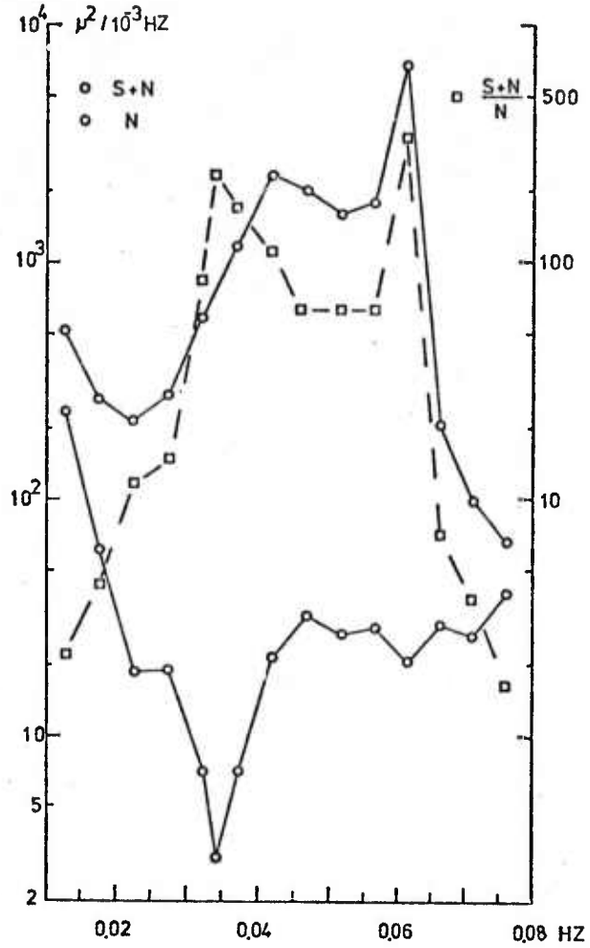


Power density spectrum for the vertical component at KIP of the Kuril Island $M_S(20)=4.5$ earthquake, 3 Oct. 1973 and a preceding equally long noise section (1024sec)(left hand scale). Squares indicate (S+N)/N ratio (right hand scale). Instrument response was included.

Fig. 2

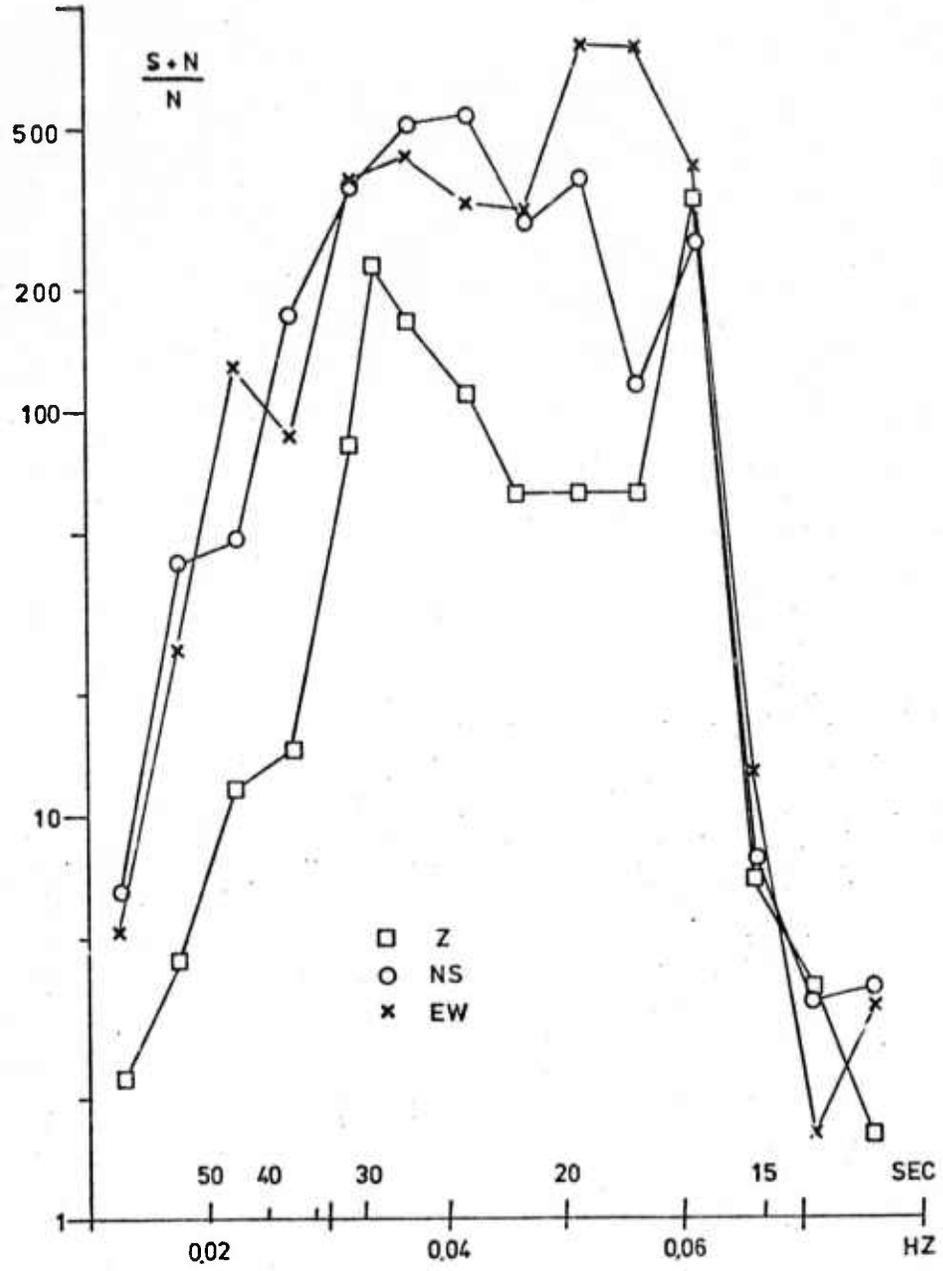


(S+N)/N power ratio for all three components of the same earthquake as in previous figure, horizontals however without instrument corrections.

Fig. 3

## II Accomplishments

The major results from the research under this grant have been either published (Berg, 1974; Berg, 1975) , are in press (Berg and Chesley, 1976; Chesley and Berg, 1976) or will be reported in the later section.

The first two publications (Berg, 1974 and 1975) essentially describe the extraction and amplitude determination from the high gain long period stations by the use of matched reference earthquake filters applied at a single station. Therefore, only the Abstract of one (Berg, 1975) is given (Section IIA).

The paper: Automated High-precision Amplitude and Phase Calibration of Seismic Systems (Berg and Chesley, 1976) will appear in the Bulletin of the Seismological Society of America (probably August 1976). As this paper is not yet available it is given in its accepted version (Sect. IIB). This method was developed to obtain accurate amplitude and phase information in view of determining spectral amplitude ratios automatically from the calibration pulses that are available on each HGLP data tape and thus making also monthly sinusoidal calibration unnecessary.

The last reference (Chesley and Berg, 1976) will be published as a Hawaii Institute of Geophysics Research report and contains the computer programs that have been developed or used under this grant on the IBM 370/158. For brevity only the abstract is given (Sect. IIC).

The section on "Beam Focusing" describes the use of the randomly spaced HGLP station network (or others) as an array to extract and determine amplitudes of Rayleigh waves from very weak events, with simultaneous identification of the event area. The individual station matched filtered outputs as obtained by the method of Berg (1974, 1975) are focused on the desired area, with an example taken from Novaya Zemlya (Sect. IID).

II A

Bulletin of the Seismological Society of America. Vol. 65, No. 6, pp. 1761–1778. December 1975

## RAYLEIGH WAVES FROM HIGH-GAIN LONG-PERIOD STATIONS: SIGNAL EXTRACTION, AMPLITUDE DETERMINATION, AND SEPARATION OF OVERLAPPING WAVE TRAINS

BY EDUARD BERG

ABSTRACT

For a signal-to-noise ratio between 0.2 and 0.1 on the original single-component records, amplitudes for Rayleigh waves over oceanic paths of 155° at station MAT and 98° at station KIP have been determined as 12 m$\mu$ and 24 m$\mu$ peak-to-peak, respectively, with a standard error of less than 11 per cent. In each case the processed correlation signal is the highest in a half-hour record. The method makes use of preliminary high-pass filtering and normalized reference earthquake-matched filtering, and takes full advantage of the well-dispersed oceanic surface wave.

The method also provides high resolution of co-located events with short time separation, or of widely spaced events with Rayleigh waves arriving nearly simultaneously at a single station, when the summed vertical and radial matched filtered components are used. Examples include: (1) clear separation and amplitude determination at stations KIP and MAT of two $M_S = 6.5$ earthquakes located 0.7° and 145 sec apart off the coast of central Chile; (2) clear separation at station KIP of a Novaya Zemlya $m_b = 4.8$ event from interfering Rayleigh waves of an $m_b = 5.0$ Kermadec Island earthquake arriving 120 to 140 sec prior to the searched event, with almost complete elimination of interference on the summed vertical and radial processed componeats; and (3) clear separation at station KIP of two co-located $m_b = 4.4$ and 4.5 earthquakes 6 min apart off the coast of Chile, with determination of their amplitudes in the presence of interfering Rayleigh waves from two central Alaska earthquakes, the first ($m_b = 4.1$) arriving 15 min prior to the first Chile Rayleigh wave and the second between the two Chile arrivals.

The single-station threshold reached (10 and 25 digital units, $p$–$p$) for stations MAT and KIP at 155° and 98°, respectively, corresponds to an $M_S = 3.3$ and probably can be improved further.

# II B AUTOMATED HIGH-PRECISION AMPLITUDE AND PHASE CALIBRATION OF SEISMIC SYSTEMS

Eduard Berg and Duncan M. Chesley

## ABSTRACT

Automated amplitude and phase response of the complete seismometer-recording system is obtained from step inputs to the calibration coil. High accuracy is achieved by summing as many pulses as desired (to eliminate background noise) by a correlation technique and subsequent Fourier analysis. The only parameters required are the seismometer mass, the Cal-coil constant (referred to the center of mass if appropriate) and current, and the precise onset time of one reference calibration current, which are all very stable over long time periods. Application to the High Gain Long Period system at KIP yields the magnification curve from only six pulses with less scatter ($< \pm 5\%$ for periods larger than 20 sec) than routine steady-state calibrations.

# INTRODUCTION

Many papers have described the calibration of seismometer systems. Three approaches have been developed: The parameter method, in which the parameters necessary for calculation of amplitude and phase response have been determined; the steady-state method, in which the amplitude and phase response is determined for discrete frequencies either by exiting the seismometer on a shake table or by the use of a calibration coil; and finally the transient method, in which amplitude and phase response from the recorded pulse on the seismogram are extracted using a step or impulse input into a calibration coil. Accurate knowlege of the response is especially necessary for research on surface wave attenuation and dispersion. Most of the more recent approaches necessitate tedious manual comparison with pre-calculated responses of calibration pulses (Espinosa et al., 1962, 1965) or very accurate measurements of phase and amplitudes (including their temperature variation) in a somewhat modified steady-state response approach (Mitronovas and Wielandt, 1975). Mitchell and Landisman (1969) also developed a least-square method to determine free period and damping constants of an electromagnetic seismograph from its calibration pulse, by weighting those frequencies that are the freest of noise and calculating the response for higher frequencies from the theory of seismometer-galvanometer systems. It seems difficult however to follow such an approach when more complicated systems are involved. Such systems might include band-rejection filters, additional electronic filters, and digital or FM long-distance telemetry to the final recording site.

In this paper the transient method is used and accurate amplitude and phase calibration can be most easily obtained where calibration pulses

recorded on a routine (day to day) basis and recording is on magnetic tape. By determination of the exact start of each individual recorded pulse by a correlation technique (Berg, 1974 and 1975), as many pulses as desired for accuracy can be summed and this sum Fourier analyzed. The parameters necessary to obtain the complete absolute response are the precise start time of one pulse (a "reference"), the mass, the calibration coil constant (referred to the center of mass if appropriate) and the applied calibration coil current of the seismometer.

It should be stressed that this method is directly applicable to the calibration of all systems equipped with a calibration coil and would be easier than the more cumbersome steady-state method. The method also can be used (with the appropriate slight modifications) in case of capacitor plate calibration devices (as used in tidal gravimeters) or weight lifts (as in the Askania-type bore hole tiltmeters) or expansion cells (and pieco electric crystals) as applied to the Verbandert-Melchior quartz tidal pendulums. The method is especially useful for remotely operating and recording systems, such as those in ocean-bottom, microearthquake, or planetary systems, since the parameters required (e.g. mass, calibration coil constant, and current) are very stable.

It also should be pointed out that the total system response is obtained, that is, from the ground motion to the final record. Such systems might include different transducers, electronic amplifiers, telemetry sections, and filters before the final record.

Since transient calibration in operational installations is performed remotely, no physical disturbance of the seismographs is required

In practice a ten-day tape from a Long Period High Gain station yields a sufficient number of pulses to obtain the response within better than 5% over the useful period range. Since the complex Fourier coefficients can be stored in the computer, a recorded event (to be analyzed) can be directly convolved to obtain ground motion.

## THEORY

A seismogram can be scanned and the start time and amplitude (with standard error) of the scanned pulse obtained by a correlation method (Berg, 1974, 1975), if a reference pulse is available with known start time. It is assumed that (as is customary in routine operation of seismograph stations) all calibration pulses are generated by the same calibration current into the coil. Beginning with the start times, all individual pulses are summed, and the resulting amplitude divided by the number of pulses used, to obtain a representative calibration pulse, thus eliminating noise by an amount that depends on the number of pulses used. This improved the high frequency calibration in long-period systems especially.

The equation of motion of the seismometer mass is given by (see Jarosch and Curtis, 1973 or Gamburzew, 1964)

$$\left( \frac{d^2}{dt^2} + 2\ \varepsilon_o \frac{d}{dt} + \omega_o^{\,2} \right) X = - \frac{d^2}{dt^2} Y \qquad (1)$$

where

$X$ = displacement of mass with respect to its frame

$T_o = 2\pi/\omega_o$ free period

$\epsilon_o$ = h $\omega_o$ damping coefficient

Y = ground displacement (positive in the same direction as X)

Consider a calibration current applied at t = 0 causing a step function in acceleration (equivalent)

$$\frac{d^2Y}{dt^2} = \frac{GI}{M} \cdot H(t) \qquad (2)$$

where

G = calibration coil motor constant (referred to the center of mass if applicable)

I = applied calibration current

M = seismometer mass

H(t) = Heaviside step function.

In most short period seismometers, the calibration coil is wound uniaxially with the transducer coil and equation (2) applies directly. In the case, where the calibration coil is physically located on the boom but away from the center of mass, (such as for most long period instruments) G has to be referred to the center of mass position and is given by

$$G = G_o \frac{r_c}{r_{cM}} \qquad (2a)$$

where

$G_o$ = calibration coil constant

$r_c$ = hinge to coil distance

$r_{cM}$ = hinge to center of mass distance.

Assuming no initial velocity or displacement of the mass and operating on the differential equation with the Laplace transform (after introduction of the acceleration term),

$$(S^2 + 2\,\epsilon_o\,S + \omega_o^{\,2})\;\bar{X}_A = -\frac{GI}{MS}\,. \tag{3}$$

This equation reduces to

$$\left[(i\omega)^2 + 2\epsilon_o i\omega + \omega_o^{\,2}\right]\bar{X}\,(\omega) = -\frac{GI}{Mi\omega} \tag{4}$$

where $\bar{X}_A(\omega)$ is the Fourier transform of the mass response to the step input in acceleration.

For a sinusoidal ground displacement of amplitude A, the differential equation yields the mass response $\bar{X}_D(\omega)$

$$\left[\,(i\omega)^2 + 2\epsilon_o i\omega + \omega_o^{\,2}\,\right]\bar{X}_D(\omega) = -\,(i\omega)^2\,A \tag{5}$$

and dividing the last equation by the acceleration response equation yields

$$\bar{X}_D(\omega) = \bar{X}_A(\omega) \cdot (i\omega)^3\,\frac{A\cdot M}{G\cdot I} \tag{6}$$

If $\bar{X}_R$ is the frequency response of the recording equipment including that of the transducer, the output response to the step input in acceleration will be $F_A(\omega) = \bar{X}_A(\omega) \cdot \bar{X}_R(\omega)$ and the response to the ground displacement will be $F_D(\omega) = \bar{X}_D(\omega) \cdot \bar{X}_R(\omega)$.

Since $F_A(\omega)$ can be obtained through Fourier analysis of the recorded output signal from the step input in acceleration, the total system response $F_D(\omega)$ to ground displacement of amplitude A

$$F_D(\omega) = F_A(\omega) \cdot (i\omega)^3 \frac{A \cdot M}{G \cdot I} \qquad (7)$$

can be calculated, provided M, G (or $G_o$, $r_c$ and $r_{cm}$), and I are measured. This is true with or without back coupling. This can also be seen by taking the approach of communication theory, and considering the seismometer-recording system as a "black box."

## APPLICATION

The method was applied to obtain the calibration in amplitude and phase for the Kipapa, Hawaii (KIP) High Gain Long Period system. A prototype of such a system was described by Pomeroy et al. (1969) and operational systems and installation techniques are described in a Lamont-Doherty Geological Observatory (1971) technical report. The KIP system (in 1974) includes a long period seismometer ($T_o \approx 30$ sec) sheltered in a pressure tank, with a coil transducer for the seismic output, coupled to a galvanometer ($Tg \approx 100$ sec) in a photo tube amplifier, and additional filters. The aim of part of the filters is to reject the predominant ocean-generated 6-sec microseisms that strongly limit the magnification of the WWSN long period components. The output is then recorded digitally. The reference pulse was obtained by summing the six pulses from Nov. 22, 24, and 26, 1974. Negative-going pulses were added with the inverse sign. The time coincidence was obtained from the start time as indicated by the station log sheet and verified by the correlation method (see later). Figure 1 shows the average pulses thus obtained for the Z (CH:S1), NS (CH:S2), and EW (CH:S3) components, where the start time

is at the minute mark labeled "2" and the y axis is labeled in digital units. Start times of the individual pulses were verified by the correlation method of Berg (1974, 1975) and are shown for the 22 Nov. pulses in Figure 2. In this figure the correlation traces are labeled CH:C_ and the time on the correlation traces is in terms of start time of the reference traces, so that maximum correlation (± 1) is at the start time of the calibration pulse in the record section. Table 1 shows the computer output data for the calibration pulse correlations for Nov. 22, 24, and 26, 1974. The time column gives the calculated start times of the calibration current; "data for maximum" refers to the positive-going pulse, and "data for minimum" to the negative-going pulse. All start times thus obtained from the correlation method are within ± 1 second (the digitizing interval) from those in the station log sheet. The column "slope" gives the relative amplitude with respect to the reference (the average of the six pulses for the particular component) "error" is one standard deviation of the "slope" (relative amplitude) and "amplitude" is the peak to trough amplitude in digital units. It can be seen from the table that with the exception of day 326, all positive-going pulses have larger amplitudes than the negative-going pulses, possibly pointing towards some instrumental asymmetry. This is also reflected in the fact that the amplitude errors (one standard deviation) are considerably smaller than the actual deviations from the average amplitudes. From statistics, one would expect a 99% confidence interval for about 2.6 standard deviations (see Crow et al., 1960, p. 160 and 231). The actual average peak to trough amplitudes (three positive- and three negative-going pulses) are: for Z, 1100.0; for N-S, 1694.7; and for E-W, 1922.0

digital units, whereas the average amplitudes of the three positive-going pulses (as obtained from the correlation output in Table 1) are: for Z, 1120.1 ± 8.8; for N-S, 1731.2 ± 69.4; and for E-W, 1948.4 ± 77.3.

The average pulses from the three components have been submitted to a fast Fourier transform to obtain the response to a step of acceleration $F_A(\omega)$ (in equation 7) and (by multiplying with $(i\omega)^3 A \cdot M/(G \cdot I)$) the displacement response $F_D(\omega)$. If the record amplitudes are measured in digital units (Dig), $\omega$ in 1/sec, A in meters, M in kg, G in Newtons/Amp (mkg/(sec$^2$Amp)) and I in Amp, the output is obtained in Dig/m.

The instrument constants applied here were supplied by John Hoffman (Albuquerque Seismological Laboratory, personal communication) and are as follows:

| | Mass (kg) | $G_o$ (Newton/Amp) | $r_c$ (mm) | $r_{cM}$ (mm) | G (calculated) $= G_o \cdot r_c / r_{cM}$ |
|---|---|---|---|---|---|
| Z | 13.2 | 0.0309 | 378 | 230 | 0.05078 |
| N-S | 10 | 0.0237 | 378 | 227 | 0.03947 |
| E-W | 10 | 0.0277 | 378 | 227 | 0.04613 |

($r_c$ = coil distance to hinge, $r_{cM}$ = center of mass distant to hinge)

and the calibration current in all cases is constant at 5 micro Amp.

The amplitude response thus obtained for the three components of the KIP High Gain Long Period instruments is shown in Figure 3. In this figure the circles represent amplitude response for a 256-sec-long section starting at the onset of the calibration current, the small crosses represent amplitude response for a 512-sec-long section starting at the

same time as the 256-sec section. It can be seen that the longer section introduces considerably more noise at shorter periods. Also shown for comparison are the steady state calibration values at 100, 70, 40, and 30 sec, obtained during the two immediately preceding routine checks on 10 Oct. and 8 Nov., 1974 (John Hoffman, personal communication). It can be seen that the analysis of the transient response of six averaged pulses results in an amplitude response within 5% of the smooth line in the worst case for periods longer than 20 seconds on the Z and EW components and longer than 24 sec for the NS component for a 256-sec record length, whereas the steady-state calibrations at 30 sec show considerably more variation (typically 10% or more). It should be pointed out that the variation obtained in the transient analysis can easily be reduced by application of more calibration pulses, especially during days when microseismic background noise is low.

The phase response of the three components is given in Figure 4. The response is smooth to the same short-period range as the amplitude response. Since the time of the calibration pulses used here the system has been changed from photo-tube amplifiers to solid state, with the solid state response to be as closely identical as possible to the older system. Jon Peterson (written communication, December 8, 1975) supplied a phase response that matches (for the N-S component) ours "perfectly" except for a factor of $\pi$ (or $180^{\circ}$). The inverse Fourier transform of our amplitude and phase response which is the time response to an impulse in ground motion in the positive direction, yields the first swing in the positive direction. Therefore the phase response presented here should be the correct one.

## DISCUSSION

The limitations of the transient calibration are given by the ratio of the cal-pulse amplitude to seismic background noise and by the accuracy in the determination of M, G (or $G_o$, $r_c$, $r_{cM}$), and I. The percentage errors in M, G, and I appear linearly in the absolute amplitude results and can be made small, and the change with time in a typical installation should be very small (< 0.1%/y). They do not affect phase or relative amplitude. The major error source then is provided by the seismic background noise, since the useful signal amplitude is fixed. As demonstrated here, the noise background can be reduced by averaging a number of pulses by a correlation technique. The advantage of the method is clear: the calibration can be performed on a routine basis automatically without physically disturbing the seismometer or the recording equipment and no other human error sources other than in the measurement of M, G, and I will occur. It is especially advantageous in remote installations where telemetry links are involved since pulses are much more easily generated and amplitude-controlled than are the sinusoidal signals used in steady state calibration, and can be applied automatically at regular time intervals. The recorded tapes of remote stations can be processed in a central location, thus avoiding displacement of personnel and equipment. Since for research the calibration can be obtained usually from the same data tape as the seismic events, it is possible to convert the trace amplitudes and phases directly to ground motion by Fourier transforming the record, dividing by the response and inverse Fourier

transform back to ground motion. Needless to say the method can also be applied to short-period and other seismic systems, recording gravimeter, and pendulum-type tiltmeters.

## ACKNOWLEDGMENTS

The authors express thanks to Jon Peterson and John Hoffman of the Albuquerque Seismological Center, New Mexico, for providing the digital tapes and seismometer parameters of the KIP High Gain Long Period station. Gratitude is also expressed to Dr. G. H. Sutton for discussions and his continuous interest in this work.

This research was supported by the Advanced Research Project Agency of the Department of Defense and was monitored by the Air Force Office of Scientific Research under Contract AFOSR 74-2612.

REFERENCES

Berg, Eduard (1974). Rayleigh waves from high gain long period stations: signal extraction; amplitude determination; and separation of overlapping wave trains, Rept. HIG-74-10, Hawaii Inst. Geophys., Univ. Hawaii, 29 pp., 21 computer outputs.

Berg, Eduard (1975). Rayleigh waves from high gain long period stations: signal extraction; amplitude determination; and separation of overlapping wave trains, Bull. Seism. Soc. Am., 65, Dec. 1975.

Crow, Edwin L., Frances A. Davis and Margaret W. Maxfield (1960). Statistics Manual, Publ. S599, Dover Publications, Inc., New York.

Espinosa, A. F., G. H. Sutton and H. J. Miller (1962). A transient technique for seismograph calibration, Bull. Seism. Soc. Am., 52, 767-779.

Espinosa, A. F., G. H. Sutton and H. J. Miller (1965). A transient technique for seismograph calibration manual and standard set of theoretical transient responses, VESIAC Spec. Rept. 4410-106-X, Geophy. Lab., Inst. Sci. Tech., Univ. Michigan.

Gamburzew, G. A. (1964). Grundlagen Seismicher Erkundung, (German Translation from the Russian by H. Bartzsch and G. Weimert) B. G. Teubner Verlagsgesellschaft, Leipzig.

Jarosch, Hans and A. R. Curtis (1973). A note on the calibration of the electromagnetic seismographs, Bull. Seism. Soc. Am., 63, 1145-1155.

Lamont-Doherty Geological Observatory (1971). High-Gain, Long-Period Seismograph Station Instrumentation, vol. 1 and 2, Advanced Research Project Agency Order 1513, 58 pp.

Lee, Y. W. (1960). Statistical Theory of Communication, John Wiley & Son, Inc., New York, London.

Mitchell, B. J. and M. Landisman (1969). Electromagnetic seismograph constants by least-squares inversion, Bull. Seism. Soc. Am., 59, 1335-1348.

Mitronovas, W. and E. Wielandt (1975). High-precision phase calibration of long period electromagnetic seismographs, Bull. Seism. Soc. Am., 65, 411-424.

Pomeroy, R. W., G. Hade, J. Savino, and R. Chander (1969). Preliminary results high-gain wide-band long-period electromagnetic seismograph systems, J. Geophys. Res., 74, 3295-3298.

TABLE 1

REF FROM 1968- 0- 0: 0: 0 TO 0- 0: 5: 0 SCAN FROM 1974-326-17:52: 0 TO 326-18:22: 0

| CHANNEL | TIME | CORR COEF | SLOPE | LOGSLOPE | ERROR | AMPLITUDE | AMP ERROR |
|---|---|---|---|---|---|---|---|
| DATA FOR MAXIMUM | | | | | | | |
| CH 1 | 1974-326-17:59: 0 | 0.9982 | 1.009439 | 0.00408 | 0.003531 | 1110.38 | 3.88 |
| CH 2 | 1974-326-17:59: 0 | 0.9929 | 1.060671 | 0.02558 | 0.011492 | 1797.48 | 19.47 |
| CH 3 | 1974-326-17:59: 0 | 0.9938 | 1.050376 | 0.02493 | 0.006878 | 2035.54 | 13.22 |
| SUM | 1974-326-17:59: 0 | 0.9916 | ********** | ******** | ********** | ********** | ********** |
| DATA FOR MINIMUM | | | | | | | |
| CH 1 | 1974-326-18:15: 0 | -0.9990 | -1.012991 | 0.00561 | 0.002596 | -1114.29 | 2.86 |
| CH 2 | 1974-326-18:14:59 | -0.9857 | -1.019055 | 0.00820 | 0.010088 | -1726.96 | 17.10 |
| CH 3 | 1974-326-18:15: 0 | -0.9936 | -1.014234 | 0.00614 | 0.006673 | -1949.36 | 12.83 |
| SUM | 1974-326-18:15: 0 | -0.9926 | ********** | ******** | ********** | ********** | ********** |

REF FROM 1968- 0- 0: 0: 0 TO 0- 0: 5: 0 SCAN FROM 1974-328-18:29: 0 TO 328-18:59: 0

| CHANNEL | TIME | CORR COEF | SLOPE | LOGSLOPE | ERROR | AMPLITUDE | AMP ERROR |
|---|---|---|---|---|---|---|---|
| DATA FOR MAXIMUM | | | | | | | |
| CH 1 | 1974-328-18:36:20 | 0.9979 | 1.025038 | 0.01074 | 0.003815 | 1127.54 | 4.20 |
| CH 2 | 1974-328-18:36:20 | 0.9980 | 1.025047 | 0.01074 | 0.003731 | 1737.11 | 6.32 |
| CH 3 | 1974-328-18:36:20 | 0.9987 | 0.999843 | -0.00007 | 0.002915 | 1921.70 | 5.60 |
| SUM | 1974-328-18:36:20 | 0.9982 | ********** | ******** | ********** | ********** | ********** |
| DATA FOR MINIMUM | | | | | | | |
| CH 1 | 1974-328-18:53:20 | -0.9978 | -0.971519 | -0.01255 | 0.003759 | -1068.67 | 4.13 |
| CH 2 | 1974-328-18:53:20 | -0.9960 | -0.959425 | -0.01799 | 0.004991 | -1625.90 | 8.46 |
| CH 3 | 1974-328-18:53:20 | -0.9994 | -0.993576 | -0.00280 | 0.001988 | -1909.65 | 3.82 |
| SUM | 1974-328-18:53:20 | -0.9977 | ********** | ******** | ********** | ********** | ********** |

REF FROM 1968- 0- 0: 0: 0 TO 0- 0: 5: 0 SCAN FROM 1974-330-17:21:28 TO 330-17:51:28

| CHANNEL | TIME | CORR COEF | SLOPE | LOGSLOPE | ERROR | AMPLITUDE | AMP ERROR |
|---|---|---|---|---|---|---|---|
| DATA FOR MAXIMUM | | | | | | | |
| CH 1 | 1974-330-17:28:28 | 0.9986 | 1.020339 | 0.00874 | 0.003158 | 1122.37 | 3.47 |
| CH 2 | 1974-330-17:28:27 | 0.9938 | 0.978934 | -0.00925 | 0.006349 | 1658.97 | 10.76 |
| CH 3 | 1974-330-17:28:27 | 0.9978 | 0.982284 | -0.00776 | 0.003771 | 1897.95 | 7.25 |
| SUM | 1974-330-17:28:27 | 0.9961 | ********** | ******** | ********** | ********** | ********** |
| DATA FOR MINIMUM | | | | | | | |
| CH 1 | 1974-330-17:39:48 | -0.9978 | -0.960626 | -0.01745 | 0.003653 | -1056.69 | 4.02 |
| CH 2 | 1974-330-17:39:40 | -0.9732 | -0.961218 | -0.01719 | 0.013139 | -1628.94 | 22.27 |
| CH 3 | 1974-330-17:39:40 | -0.9860 | -0.952472 | -0.02115 | 0.009949 | -1830.65 | 19.20 |
| SUM | 1974-330-17:39:39 | -0.9838 | ********** | ******** | ********** | ********** | ********** |

## FIGURE CAPTIONS

Figure 1. Average of the three positive-going and the three inverted negative-going calibration pulses of station KIP for Nov. 22, 24, and 26, 1974; upper trace, vertical; middle trace, N-S; bottom trace, E-W. Amplitudes are in digital units (y-axis) and time is in minutes (x-axis).

Figure 2. Lines 3, 6, and 9 are the average of six calibration pulses of the vertical, N-S, and E-W components (the reference pulses). Lines 2, 5, and 8 are the seismograms for Nov. 22, 1974. Amplitudes are in digital units, time ticks are 2 minutes apart. Lines 1, 4, and 7 are the correlation between the reference pulse and the seismogram for the vertical, N-S, and E-W components. Amplitudes are the correlation coefficients (from +1 to -1). The maximum and minimum of these traces occur at the time of calibration-pulse onset (given in Table 1).

Figure 3. Amplitude response of the KIP High Gain Long Period system obtained by Fourier transform of the average of six calibration pulses for the vertical (3A), the N-S (3B), and E-W (3C) components. Note the scatter of the two steady state calibrations at 30-sec period immediately preceding the time of the present transient calibration. Reliable calibration (with less than 5% amplitude scatter) is obtained for a 256-sec-long record section for periods longer than 20 sec for the Z and E-W component, and for periods longer than 24 sec for the N-S component.

Figure 4. Phase response of the KIP High Gain Long Period System obtained by Fourier transform of the average of six calibration pulses for the (4A) vertical, the (4B) N-S, and the (4C) E-W components.

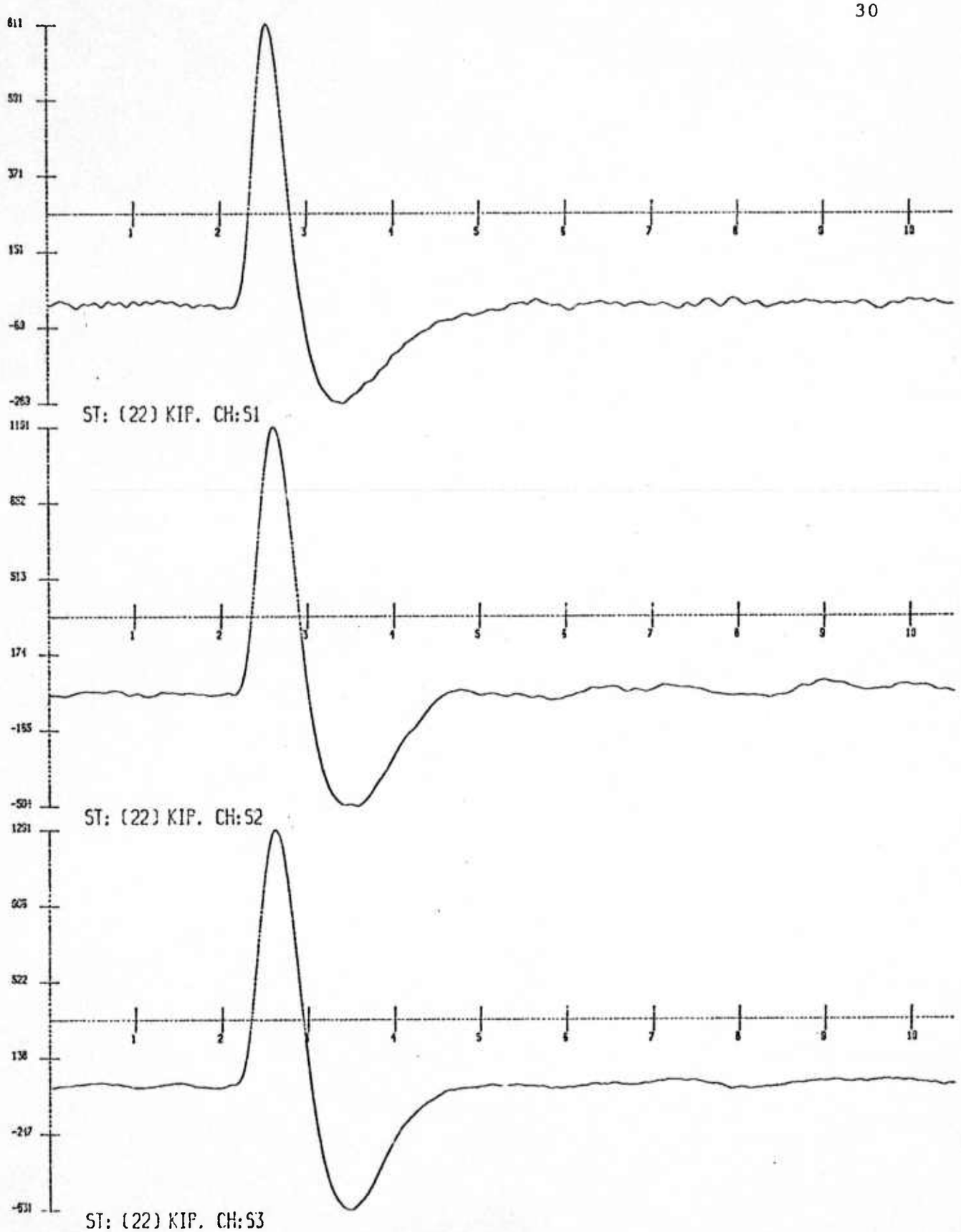


FIG. 1

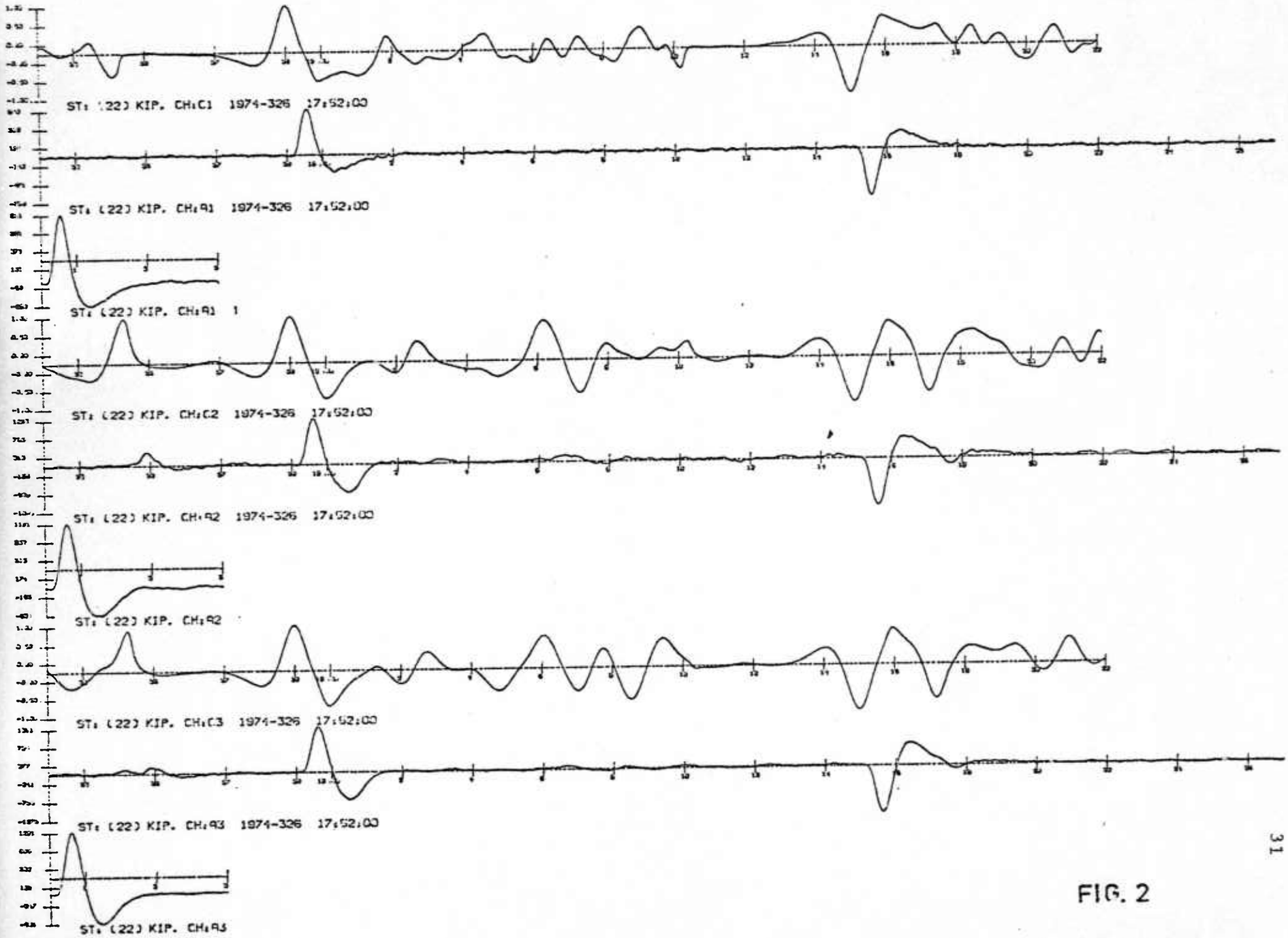
ST: (22) KIP. CH:C1 1974-326 17:52:00
ST: (22) KIP. CH:A1 1974-326 17:52:00
ST: (22) KIP. CH:A1 1
ST: (22) KIP. CH:C2 1974-326 17:52:00
ST: (22) KIP. CH:A2 1974-326 17:52:00
ST: (22) KIP. CH:A2
ST: (22) KIP. CH:C3 1974-326 17:52:00
ST: (22) KIP. CH:A3 1974-326 17:52:00
ST: (22) KIP. CH:A3

FIG. 2

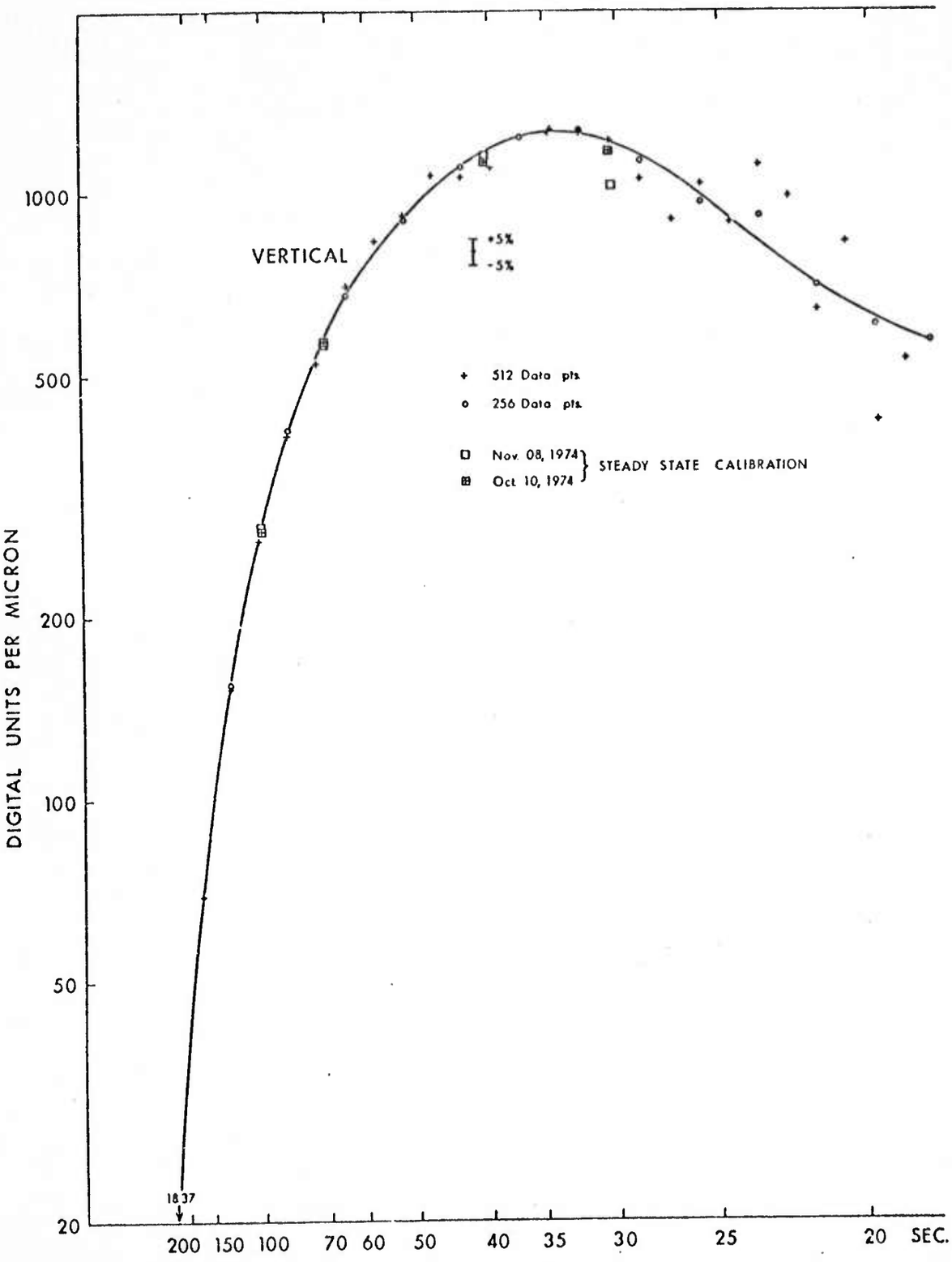
VERTICAL
+5%
-5%
512 Data pts.
256 Data pts.
Nov. 08, 1974
Oct 10, 1974
STEADY STATE CALIBRATION
DIGITAL UNITS PER MICRON
1000
500
200
100
50
20
18.37
200 150 100 70 60 50 40 35 30 25 20 SEC.

FIG. 3A

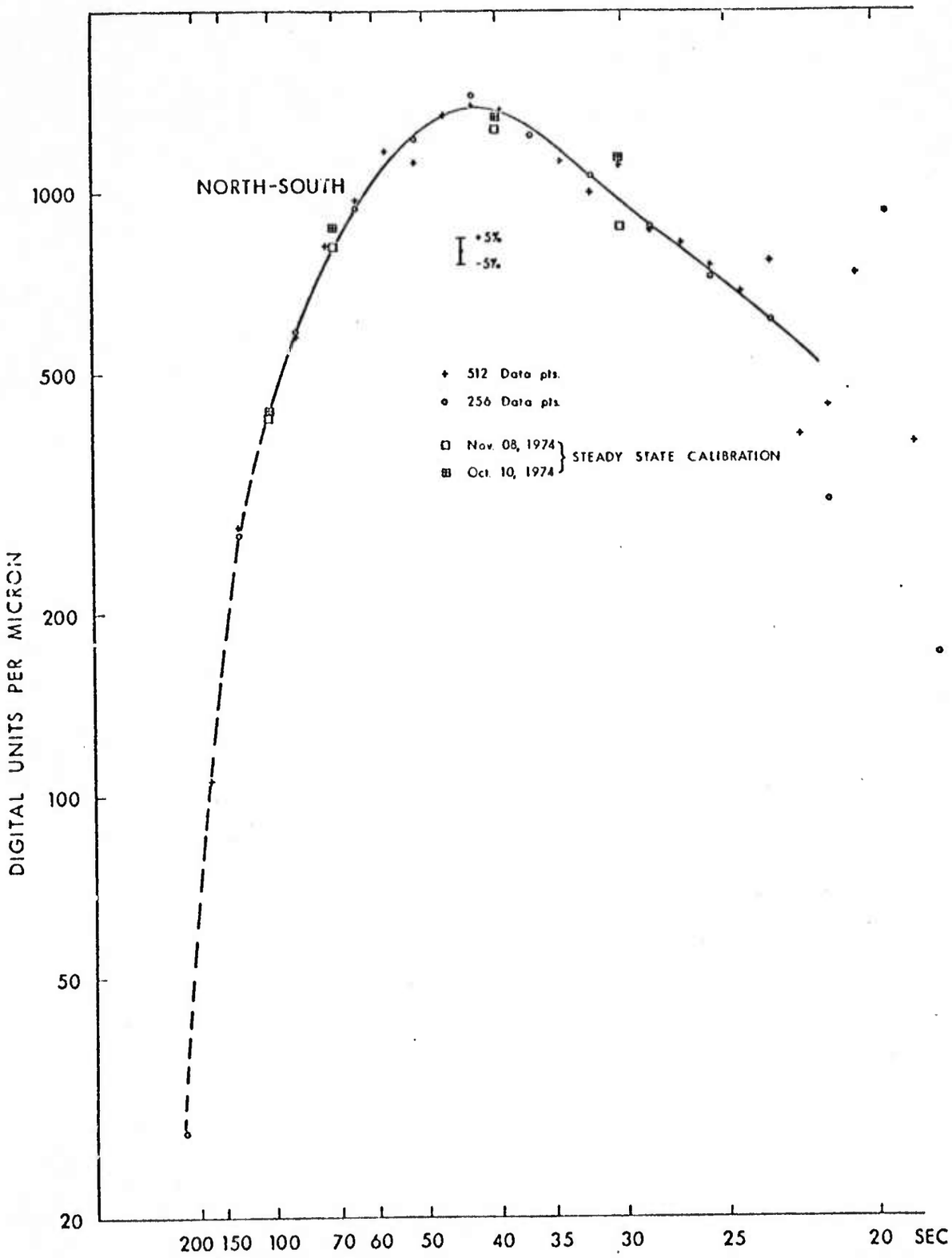
NORTH-SOUTH
+5%
-5%
512 Data pts.
256 Data pts.
Nov. 08, 1974
Oct. 10, 1974
STEADY STATE CALIBRATION
DIGITAL UNITS PER MICRON
1000
500
200
100
50
20
200 150 100 70 60 50 40 35 30 25 20 SEC

FIG. 3B

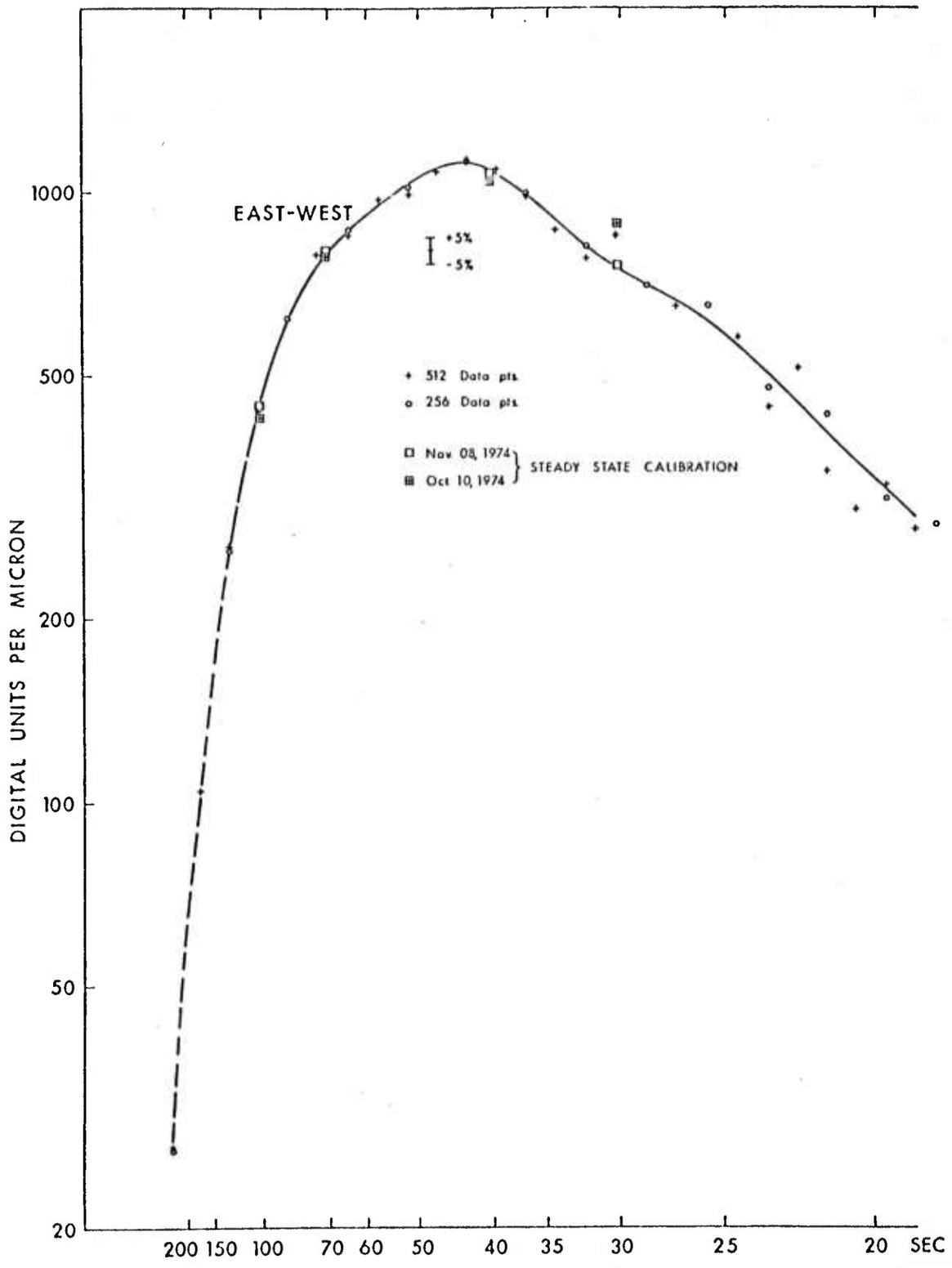
EAST-WEST
+5%
-5%
512 Data pts.
256 Data pts.
Nov 08, 1974
Oct 10, 1974
STEADY STATE CALIBRATION
DIGITAL UNITS PER MICRON
1000
500
200
100
50
20
200 150 100 70 60 50 40 35 30 25 20 SEC

FIG. 3C

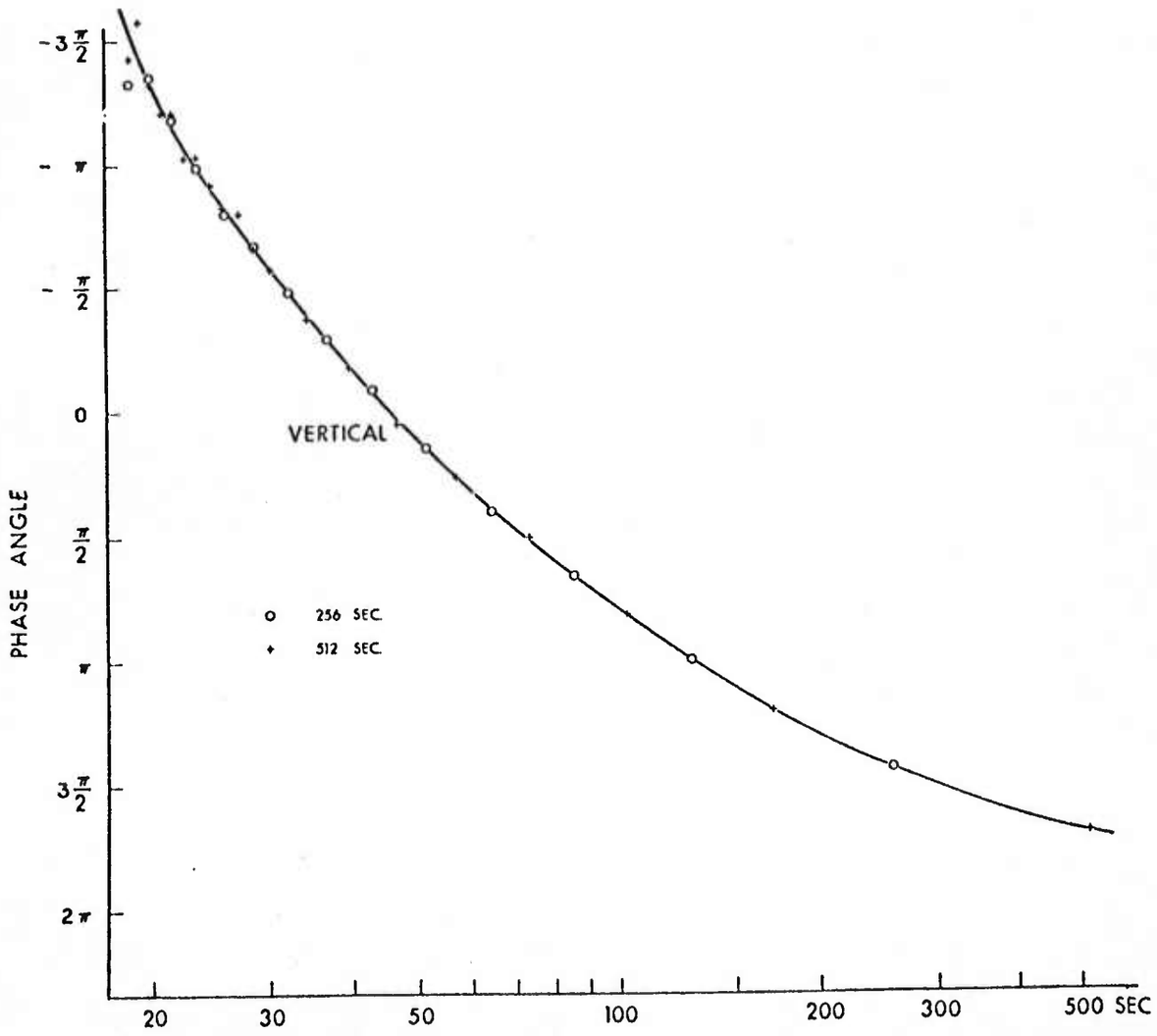
PHASE ANGLE
-3π/2
-π
-π/2
0
π/2
π
3π/2
2π
VERTICAL
o 256 SEC.
+ 512 SEC.
20
30
50
100
200
300
500 SEC

FIG. 4A

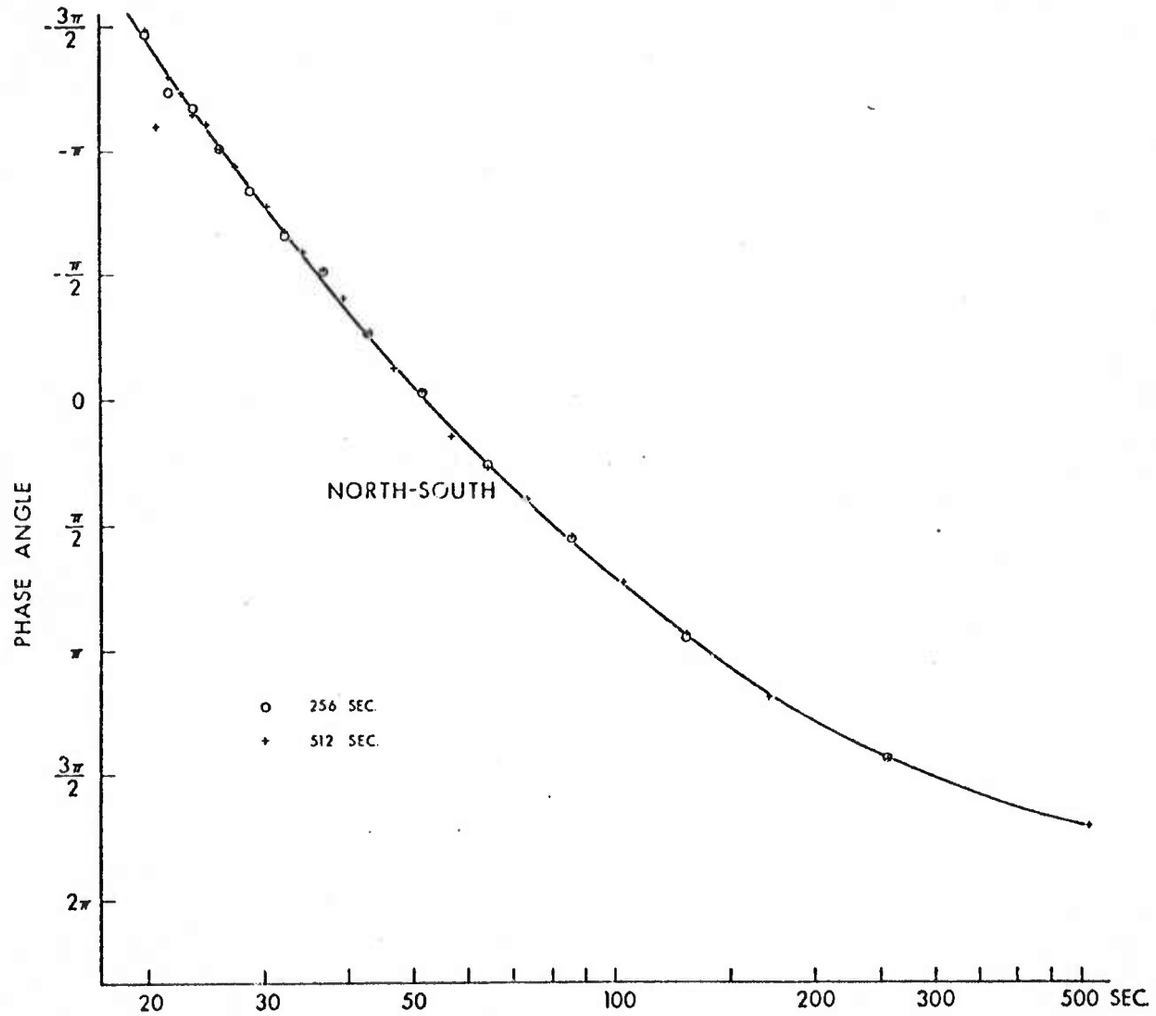
PHASE ANGLE
$-\frac{3\pi}{2}$
$-\pi$
$-\frac{\pi}{2}$
0
$\frac{\pi}{2}$
$\pi$
$\frac{3\pi}{2}$
$2\pi$
NORTH-SOUTH
o 256 SEC.
+ 512 SEC.
20
30
50
100
200
300
500 SEC.

FIG. 4B

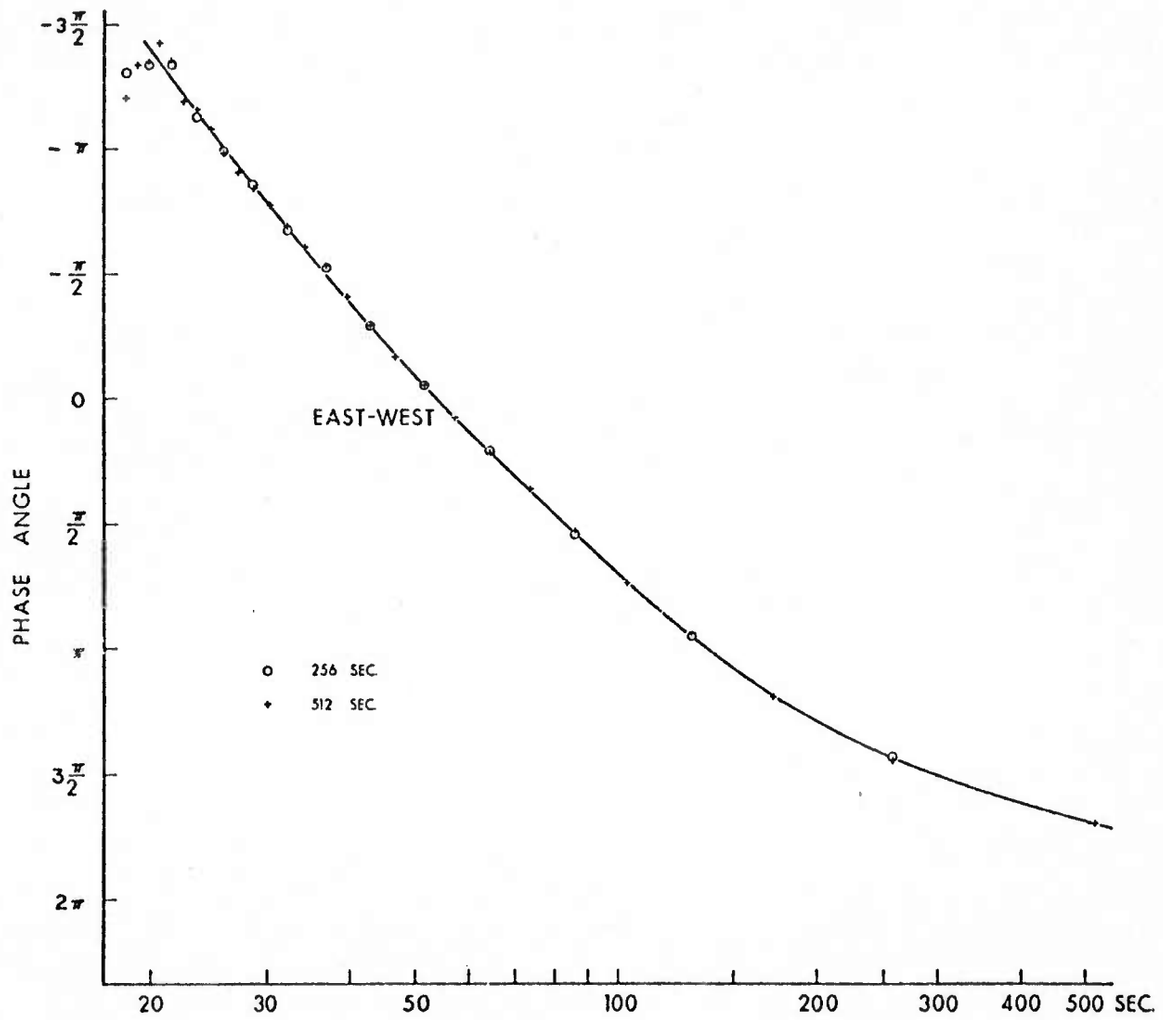
PHASE ANGLE
$-3\frac{\pi}{2}$
$-\pi$
$-\frac{\pi}{2}$
0
$\frac{\pi}{2}$
$\pi$
$3\frac{\pi}{2}$
$2\pi$
EAST-WEST
256 SEC.
512 SEC.
20
30
50
100
200
300
400
500 SEC.

FIG. 4C

II C

# Computer Programs for Seismology: Special Applications to the High-Gain Long Period Seismic Network

by

Duncan M. Chesley and Eduard Berg

Abstract:

This report describes several IBM 370/158 compu er programs that have been applied to long period seismic data on digital tapes. Included are reading routines for tapes generated by the High-Gain Long Period (HGLP) stations, rotation of the horizontal components, low-, band- and high-pass digital filters, correlation (or matched filtering), summation of correlations, beam focusing, and ground motion retrieval.

Results of applications, described elsewhere or in preparation, include extraction and amplitude determination of Rayleigh waves with signal-to-noise ratios near 1 to 10, precision amplitude and phase calibration of entire seismic systems from transducer to final record, beam forming of matched filtered outputs from the randomly spaced HGLP station array, and separation of co-located multiple events with time spacing as short as 150 sec or separation of events widely spaced geographically but arriving nearly simultaneously at a given station.

Report: HIG 76-3 estimated 75 pages, March 1976, Hawaii Institute of Geophysics, Univ. of Hawaii, in press.

## II D

## Beam Focusing of the High-Gain Long-Period Stations

The method (Sect II A) of extracting well dispersed Rayleigh waves with amplitudes far down in the noise level worked well at individual stations and especially when applied to wave trains predominantly travelling a long oceanic path. It also was argued (Berg, 1975) that slight differences in earthquake focal mechanism, focal depth or location between the reference earthquake and the extracted one would deteriorate the correlation, since the frequency-time functions of the received signals are somewhat different (besides the amplitude scaling factor). A corollary increase in the standard deviation of the amplitude determination will result.

It was thought then, that using a number of n stations and adding their correlation signals would result in an increase of the signal to noise ratio by a factor of $\sqrt{n}$ . It was found that this is nearly correct, however usually there seem to be one or two stations that show exceptionally clear correlation whereas the others are nearly at the same time, but their amplitudes are those of the noise background. As an example we have chosen the 27 Nov 1973 Novaya Zemlya explosion as a reference, to scan the records of several other stations for aftershocks or cavity collapse. Table 1 gives the source data.

Figure 1 shows the azimuthal distribution and distances (in km) of some HGLP stations with respect to the reference event of 27 November 1973. In addition, the great circle path directions of arrival for the waves are indicated by the short arrows near each station abbreviation. In Figure 2, the lower record sections are the average matched filtered output from

individual stations (marked CH:SM) given in Figure 3 and the uppermost trace is the average of the lower ones for the time interval common to all lower traces. Note the different start times of individual station traces. Since the timing of the matched filter output has been referred to the origin time (rather than the start of the Rayleigh wave) of the reference event, the correlation for the extracted event appears at its own origin time (or slightly offset if the epicenter is not the same as for the reference). The origin time for the reference event that was used here was 07:00:00, the average between the NOAA time and that in the NORSAR bulletin. The beam minimum is at 09:13:50 in good agreement with the NOAA value of 09:13:51* (see table 1).

The beam output has about twice the amplitude of the "background." We therefore expect that it is possible to further lower the detection (and proper location) threshold, and still be able to determine the average surface wave amplitude as well. Note also that the correlation "noise" for individual stations is near 0.2 whereas the beam shows the reduction by the square root of the number of stations used. The left side of Figure 2 shows the beam for only those stations, where the individual vertical, the radial or both components had detected the presence and determined the amplitude of the surface (Rayleigh) waves. The right side has the station CHG added where detection was not achieved (or was somewhat early). Obviously, if an event was detected by short period seismometers, one is in the favorable position to choose only those LP stations that have "detected" the surface waves for amplitude determination, and then for the focused beam to confirm the location. In our example neither ALQ (Fig. 3E) nor CHG (Fig. 3D) had given a single component correlation that would have been useful for

amplitude determination. Figures 3A through 3C give the individual station outputs for KIP, TLO and MAT, where at least one component succeeded in extracting the signal. Note the clear detection at KIP, Figure 3A and on the TLO vertical (second trace, Fig. 3B) and the MAT N-S (fifth trace, Fig. 3C). Table 2 summarizes the results of the detection at individual stations, for the beam focusing for the stations KIP, TLO, MAT and the beam focusing for the stations KIP, TLO, MAT, and CHG. The origin times, correlation coefficients, p-p amplitudes and magnitude differences are those obtained by the computer printout.

As the table shows the average surface wave magnitude difference for the Novaya Zemlya event is 2.29 below the reference of $M_s$ = 5.5 resulting in an $M_s$ = 3.2 and all determinations are within ± 0.1 magnitude of that value, despite the presence of interfering Rayleigh waves from an $m_b$ = 5.0 earthquake S of Kermadec (see Berg, 1975, Fig. 10). Note that the signal levels are lower than the noise level for this extracted and amplitude determined event (see Figs. 3A-D) and correspond roughly to the 50 to 60% (all event) detection level of the three stations as determined by Lambert, Brahl and Straus (November 1973). The clearly negative correlation of KIP and the beam outputs in Figure 3A and Figure 2 together with the position ($M_s$ = 3.2, $m_b$ = 4.6 LASA and BMO) on the $M_s$ - $m_b$ plot for the area presented by Savino et al. (1971, p. 8014) identify this event as earthquake or collapse.

All seismic traces in Figure 3 had been high pass filtered to eliminate the long period portion of the spectrum where noise is usually high and no significant signal is expected for very small events (see also Section I).

The question arises why detection has not been achieved at some of the stations, notably CHG, which is at the shortest distance from the epicenter. Part of the answer is probably found in the complicated spectra of the reference event, as received at the stations. These amplitude spectra have been determined for the first 512 sec of the reference event without prefiltering or corrections for instrument response and normalized to "one" at 42.7 sec. These spectral amplitude ratios are shown in Figures 4A through 4E for the stations KIP, TLO, MAT, CHG and ALQ. The high frequency cutoff is due in part to the cutoff in time of the lower velocity (higher frequency) portion of the dispersed Rayleigh wave train. It seems as if detection and amplitude determination is most easily achieved where the spectral amplitude ratio A(T)/A(42) is relatively high (above 1.6) and relatively smooth (as a function of period) in the most useful period range. These cases also seem to correspond to paths that are the least complicated in terms of lithospheric structure. Perhaps detection and amplitude determination could be achieved for the event at CHG and ALQ by first band pass filter the records around 70 and 35 sec at CHG (Fig. 4D) and ALQ. The rather strong long period parts of the station CHG and to some extend ALQ thus seem to confirm the presence of a continental type wave guide that has been used by McDonald et al. (1974) for detection of weak central Asian events.

# REFERENCES

Berg, Eduard (1975). Rayleigh waves from high-gain long-period stations: Signal extraction; amplitude determination; and separation of overlapping wave trains, Bulletin of the Seismological Society of America, 65, 6, 1761-1778.

Lambert D. G., S. R. Prahl and A. C. Strauss (1973). Evaluation of the noise characteristics and the detection and discrimination capabilities of the very long period experiment (VLPE) single stations and the VLPE Network, Special Report No. 14, Extended Array Evaluation Program, Texas Instruments, Inc., P. O. Box 6015, Dallas, Texas, 75222.

McDonald, John A., William Tucker, and Eugene Herrin (1974). Matched filter detection of surface waves of period up to 75 seconds, generated by small earthquakes, Bull. Seismol. Soc. Amer. 64, 1843.

Savino, J., L. R. Sykes, R. C. Liebermann and P. Molnar (1971). Exitation of seismic surface waves with periods of 15 to 70 seconds for earthquakes and underground explosions, J. Geophys. Res. 76, 8003-3020.

Table 1.

Source Data 27 Oct 1973 (day 300)

| | | | | | Depth | $m_b$ | $M_s$ | |
|---|---|---|---|---|---|---|---|---|
| NOAA | 0 = 06 59 57.4 | 70.8N | 54.2E | | OG | 6.9 | 5.5 | Reference event |
| NORSAR | 07 00 03 | 71 | 52 | | | -- | -- | |
| LASA | | 70 | 57 | | | 7.4 | | |
| NOAA | 09 13 51.3* | 71.3 | 51.9 | | OG | 4.8 | | Scanned event |
| NORSAR | 09 13 58 | 72 | 52 | | | 3.8 | | |
| LASA | | 70 | 56 | | | 4.6 | | |
| BMO | | | | | | 4.6 | | |
| NOAA | 09 25 46.1 | 33.7S | 179.4E | | N | 5.0 | | Earthquake interfering at KIP from S of Kermadec |

Table 2.

Computer Extracted Origin Time and Magnitude Relative to Main Event
from HGLP Stations 27 Oct 1973

| Station | HP Filt. (sec) | Comp. | Origin Time* | Correlation | p-p Amplitude (dig units) | Mag. Diff. | Mag. (5.50 + diff.) | Remarks |
|---|---|---|---|---|---|---|---|---|
| KIP | 45 | Z | 09 13 50 | -0.37 | 27 | -2.33 | 3.17 | Determined despite interference from S of Kermadec $m_b$ = 5.0 quake |
| | 45 | NS | 52 | -0.48 | 41 | -2.16 | 3.34 | |
| | | average(SM) | 51 | -0.42 | | | | |
| TLO | 50 | Z | +9 | -0.37 | 44 | -2.35 | 3.15 | Rad: Not eorreetly extracted |
| | 50 | Rad. | | | | | | |
| | | average(SM) | 49 | -0.18 | | | | |
| MAT | 55 | Z | | | | | | Z: Not correctly extraeted |
| | 55 | NS | 47 | -0.36 | 53 | -2.31 | 3.19 | |
| | | average(SM) | 50 | -0.17 | | | | |
| Beam | (average of SM traces) | | | | | | | |
| | KIP, TLO, MAT | | 09 13 50 | -0.255 | | | | |
| | KIP, TLO, MAT, CHG | | 09 13 50 | -0.170 | | | | |
| Average difference in magnitude to main event: | | | | | | -2.29 ± 0.09 | | |

*Origin time for referenee used was 07:00:00

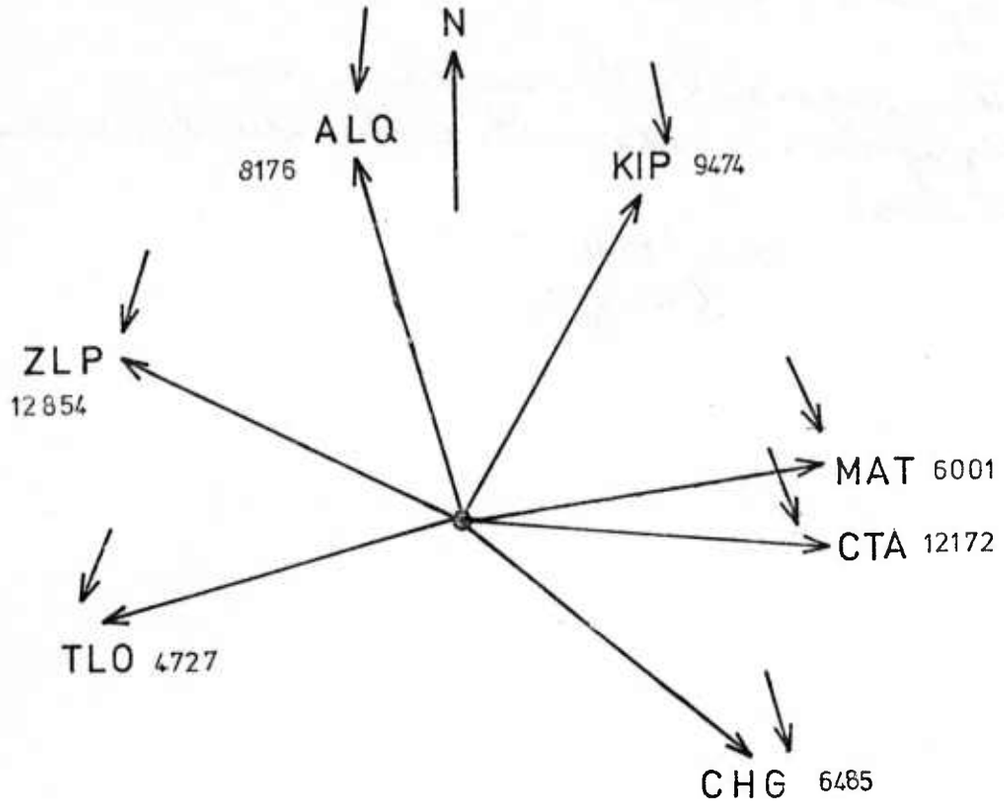


Fig. 1. Azimuthal distribution, distances and great-circle path direction of arrivals for the Nov. 27, 1973 Novaya Zemlya explosion.

46a

Pages 47 thru 57 - best available

The ups and downs have more significance than the captions under each.

per AFOSR.

DDC-TCA
6 Aug 76

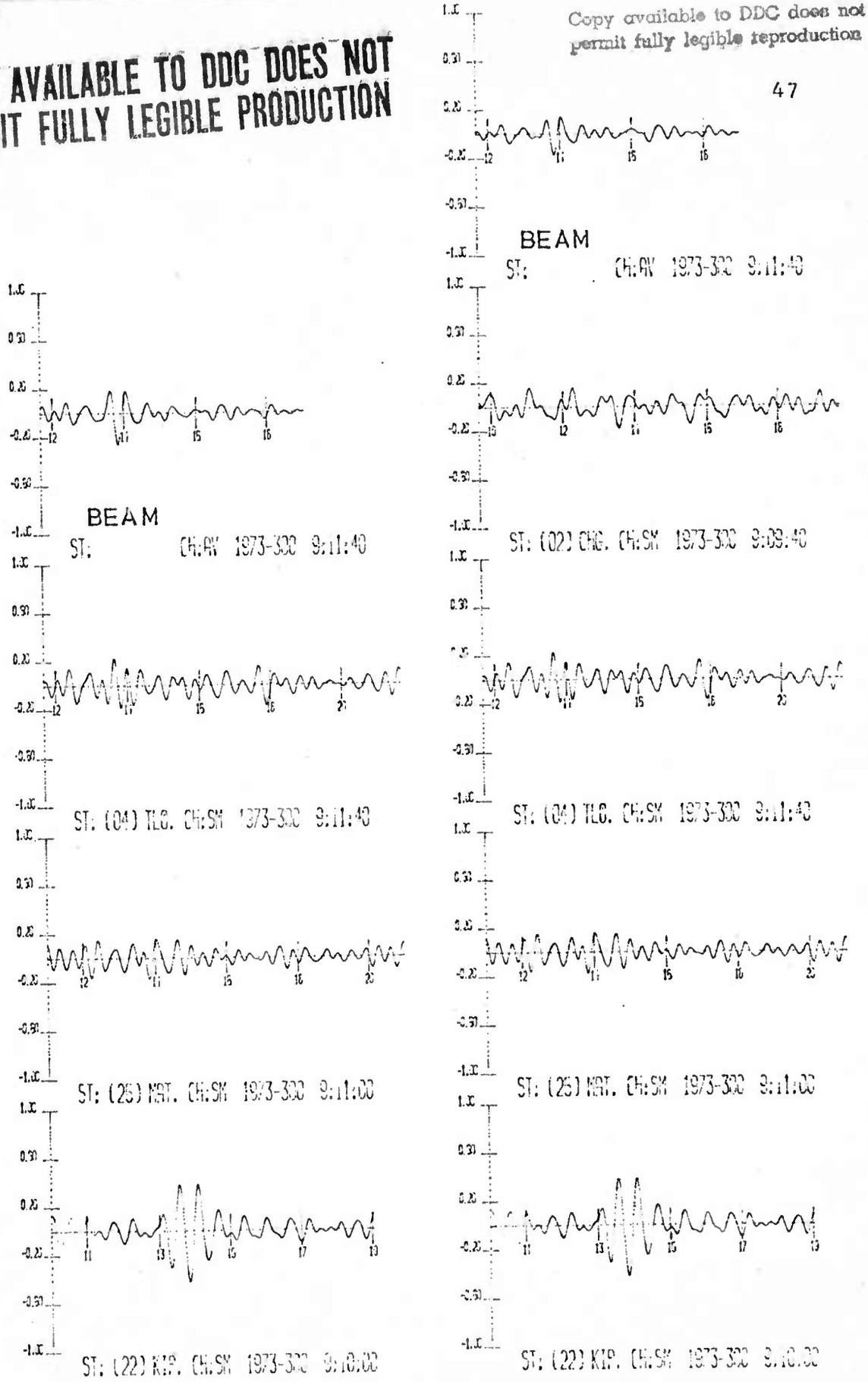


Fig. 2. Upper trace beam output, the average sum of the lower traces, which are the individual station SM traces of Fig 3. The negative correlation (with respect to the explosion waves used as reference) indicates that the event was not an explosion and gives the original time as 09:13:50 and the location near the reference event.

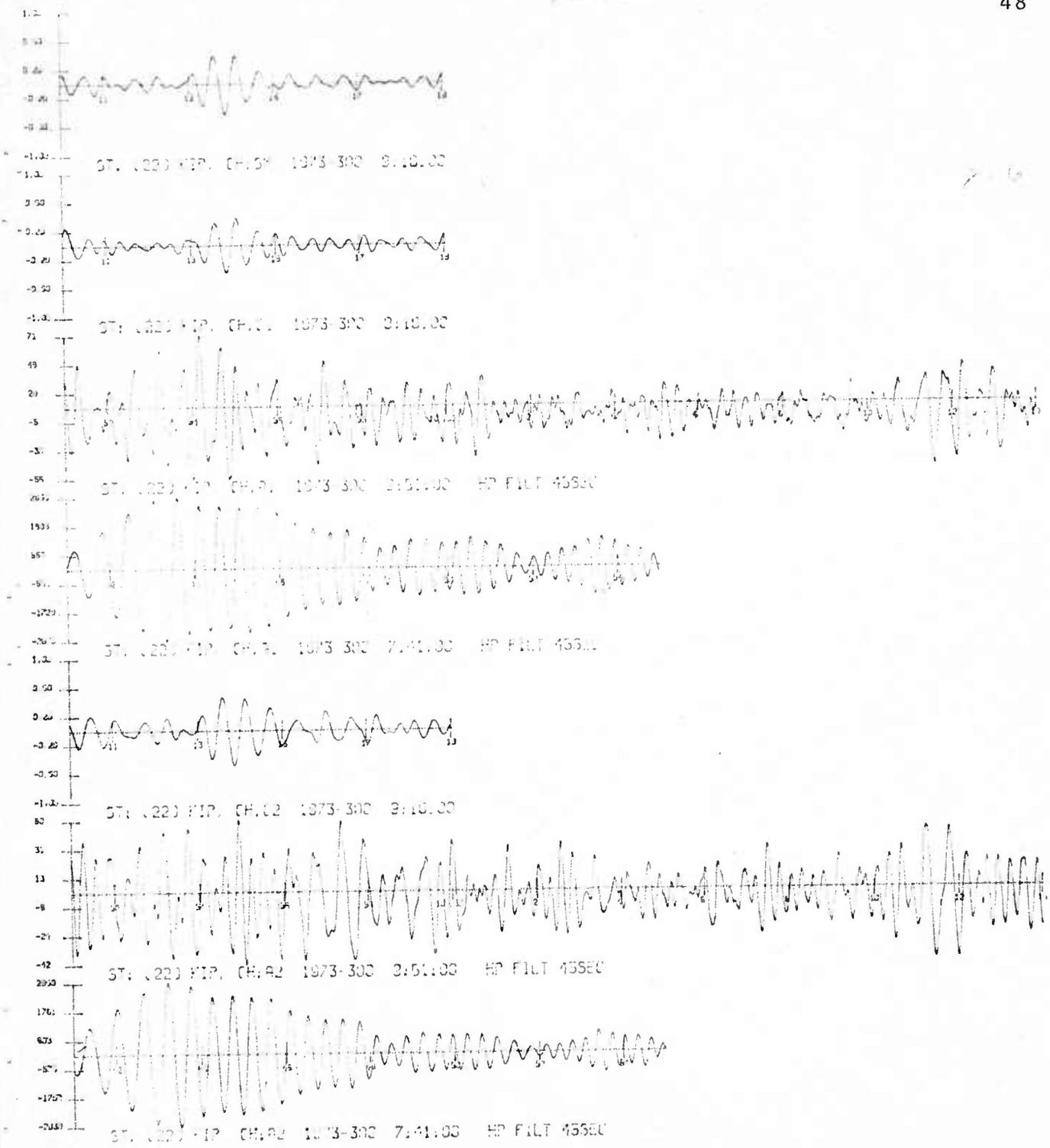

Fig. 3A. KIP - trace 1: average sum (SM) of correlation traces, note negative peak at 09:13:51; trace 2: 5 matched filter outputs (C1, C2) for the vertical and N-S (radial) components; trace 3: 6 scanned data after HP prefiltering at 45 sec (A1, A2) for the vertical, N-S component; trace 4: 7 reference explosion Rayleigh waves prefiltered (HP 45 sec) (A1, A2) for the vertical and N-S (radial) components. For values of correlation, exact time and amplitude determination see Table 2.

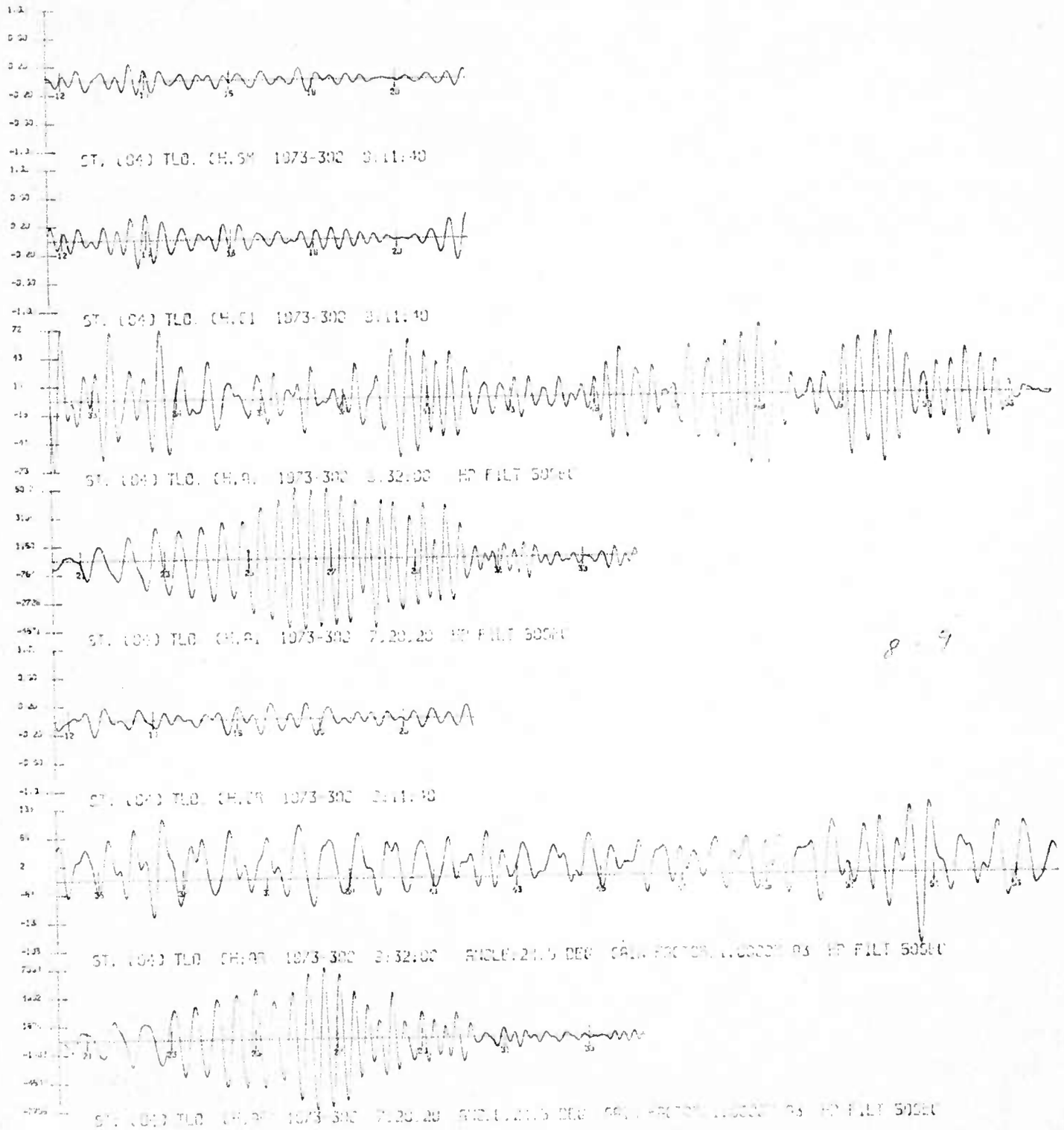

Fig. 3B. TLO for trace identification see Fig. 3A.

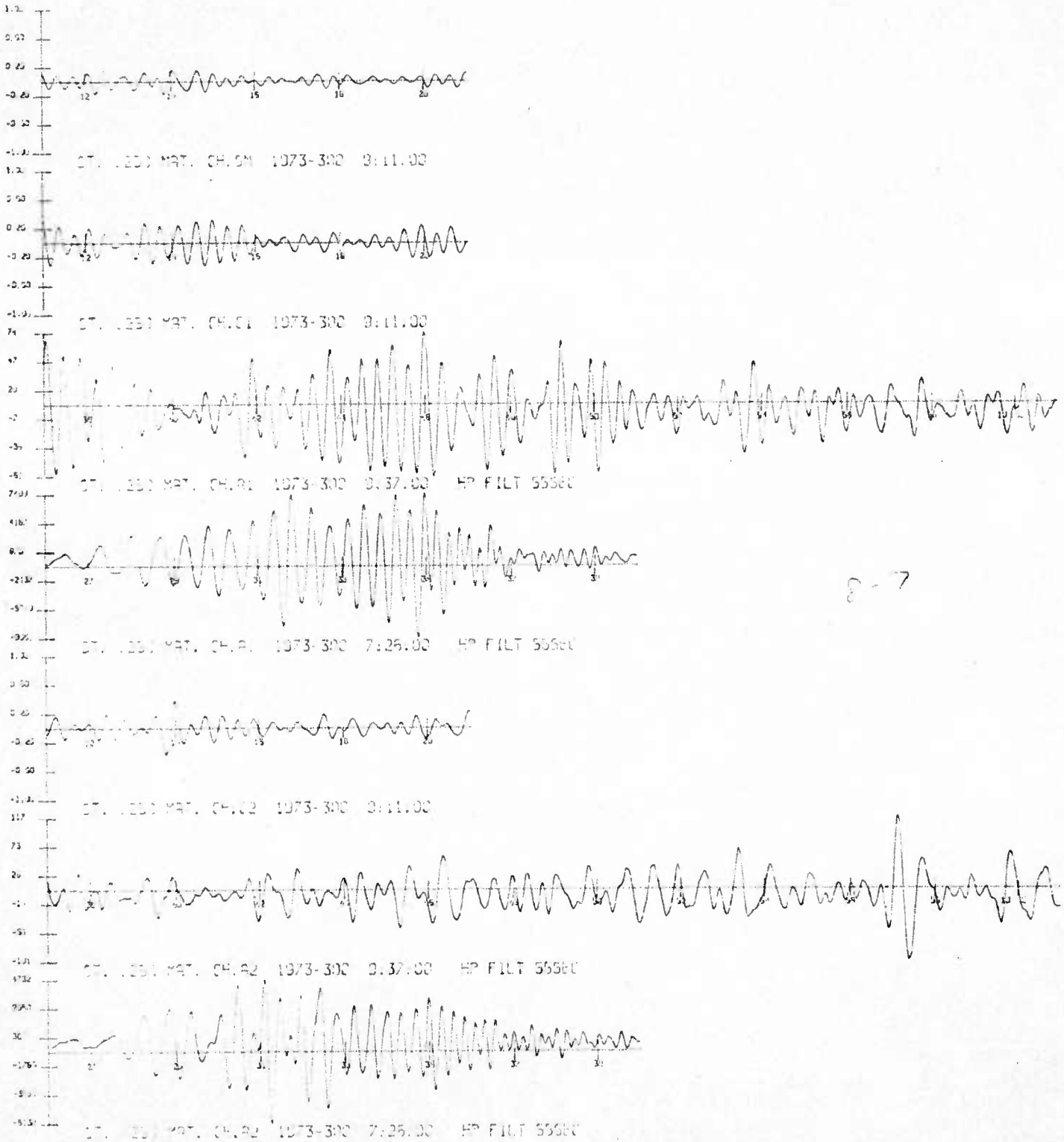

Fig. 3C. MAT for trace identification see Fig. 3A.

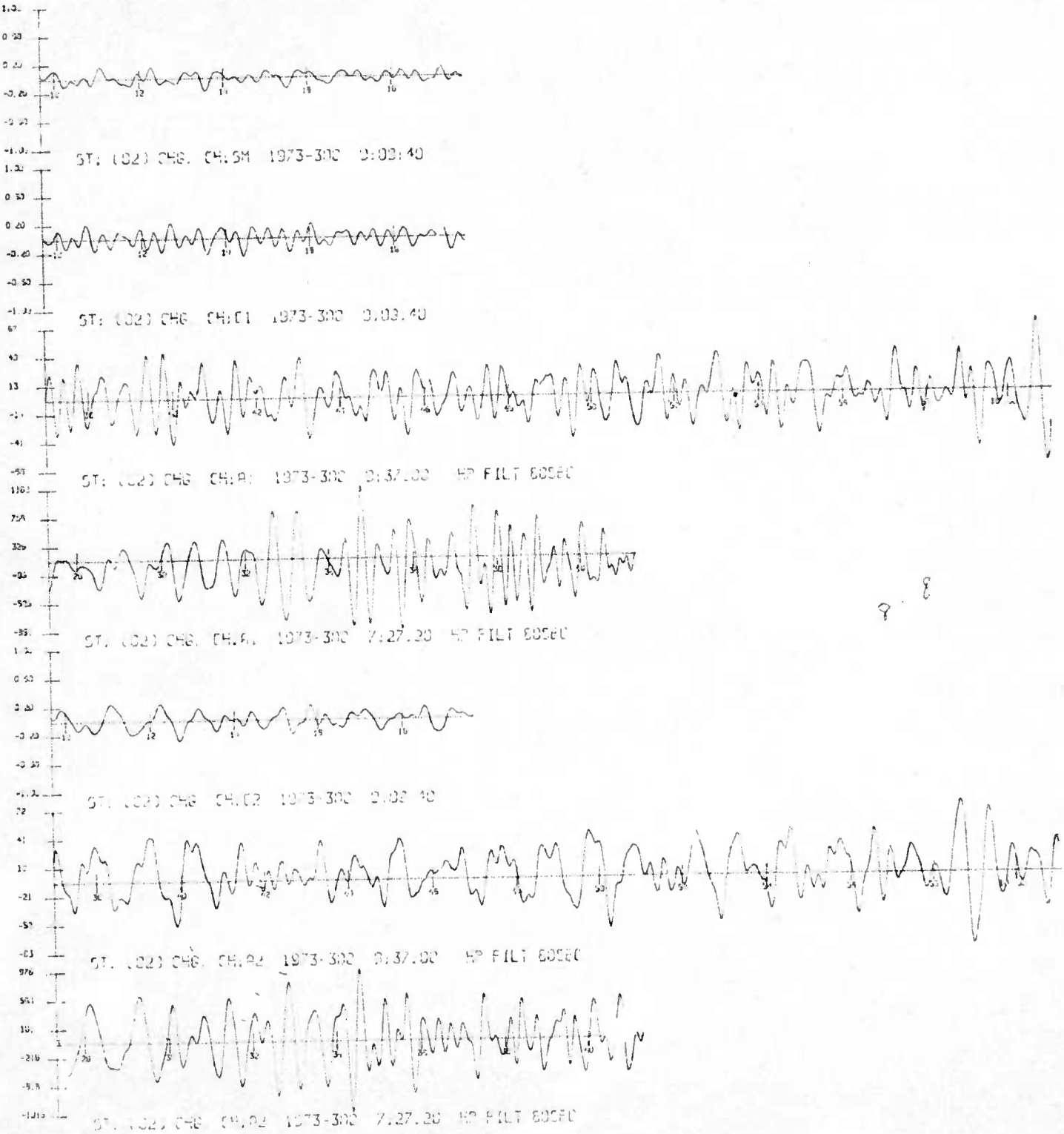

Fig. 3D. CHG for trace identification see Fig. 3A.

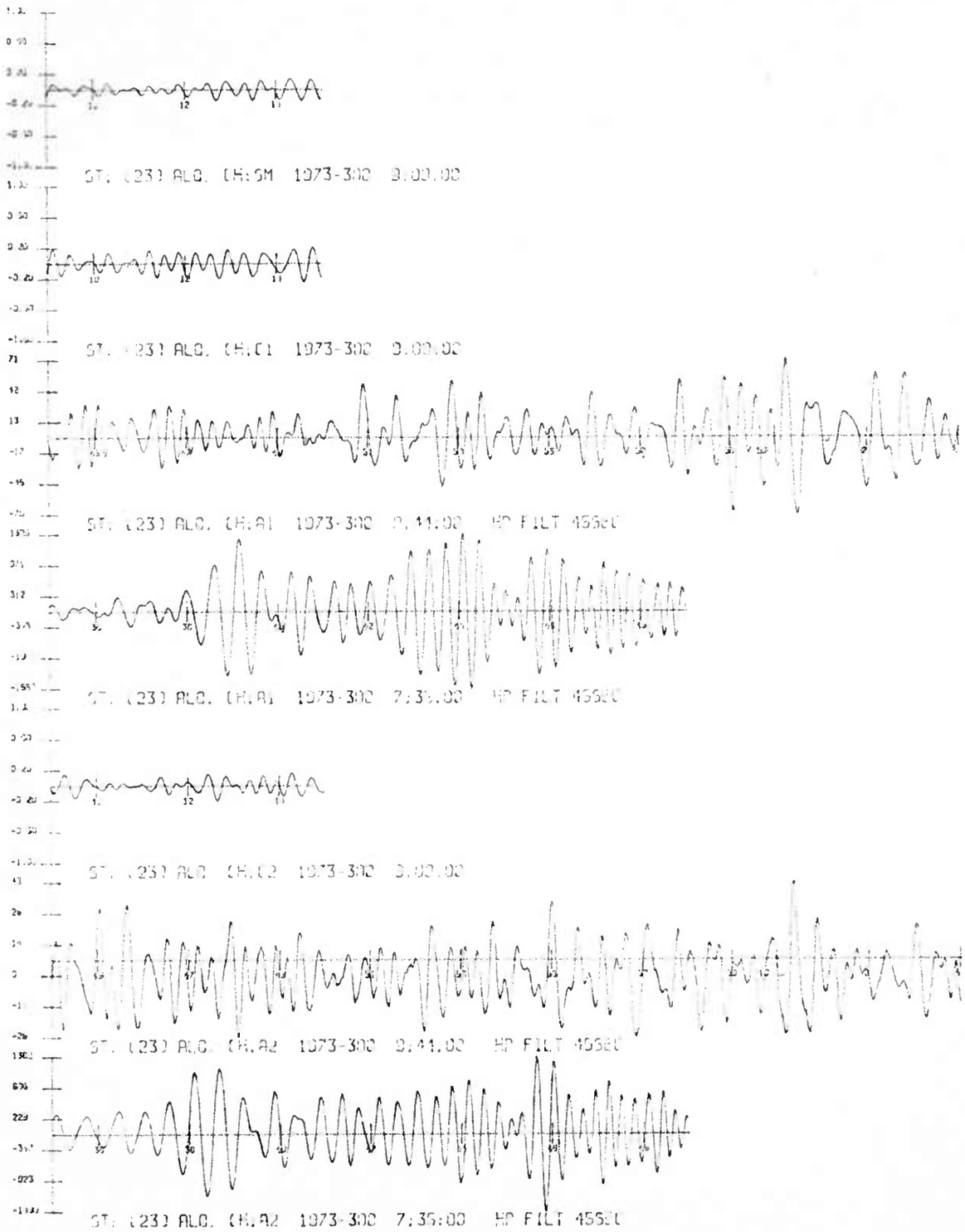


Fig. 3E. ALQ for trace identification see Fig. 3A.

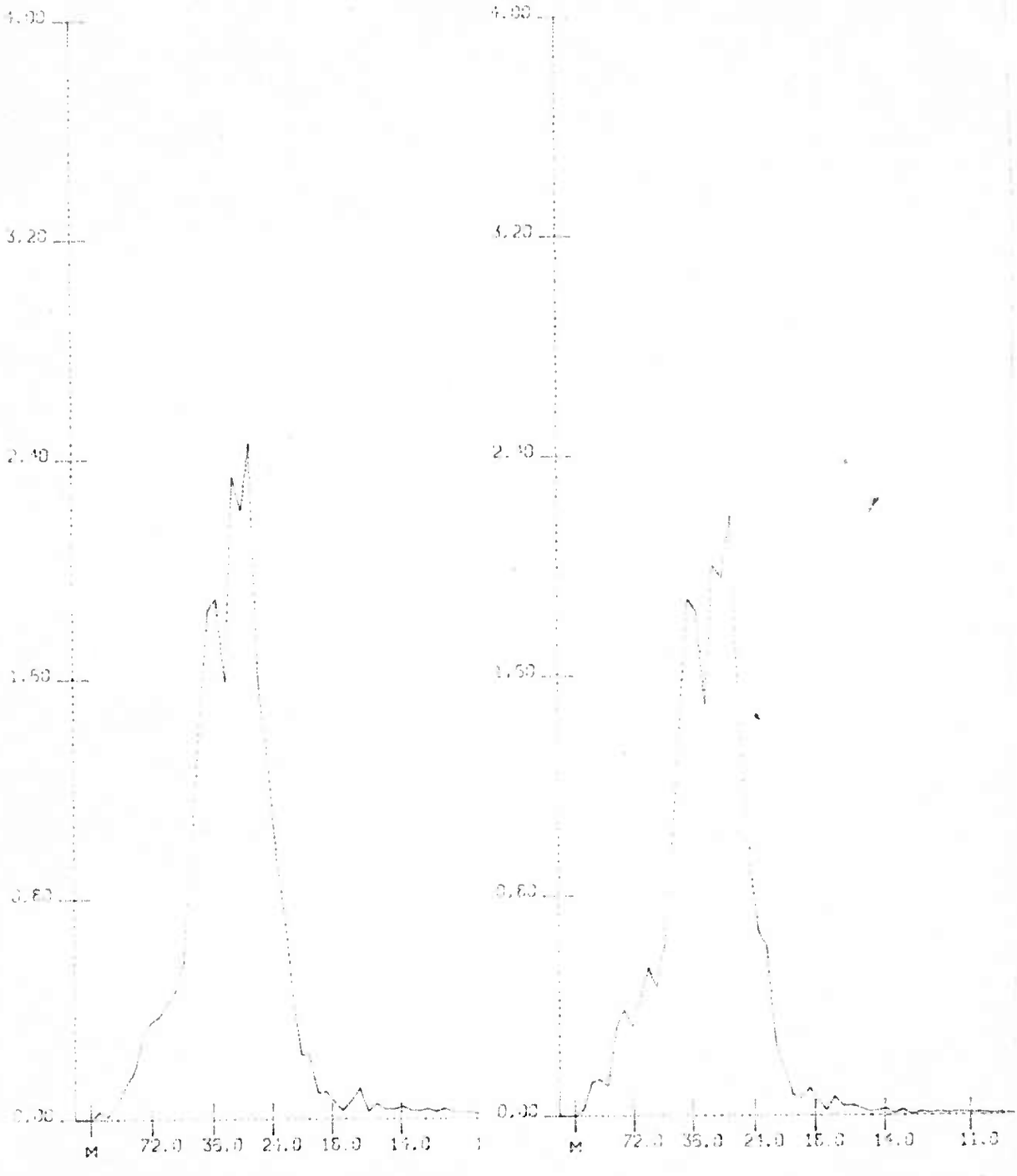


Fig. 4A. KIP: Vertical and N-S Spectral Amplitude ratios, normalized at 42.7 sec. Novaya Zemlya Start Time 7:38:55, Data length 512 sec.

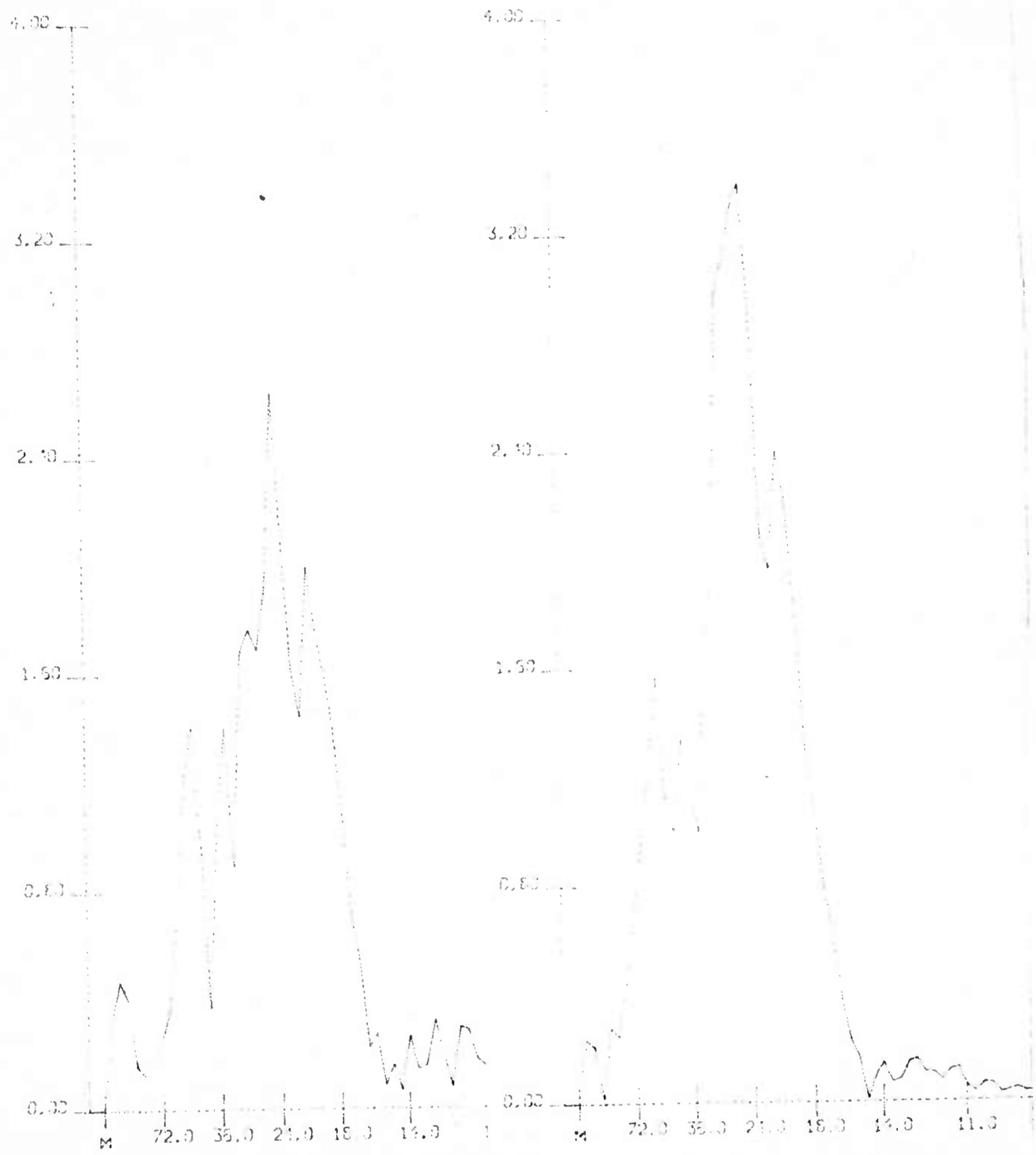


Fig. 4B. TLO: Vertical and Radial Spectral Amplitude ratios, normalized at 42.7 sec., Novaya Zemlya Start Time 7:13:00, Data length 512 sec.

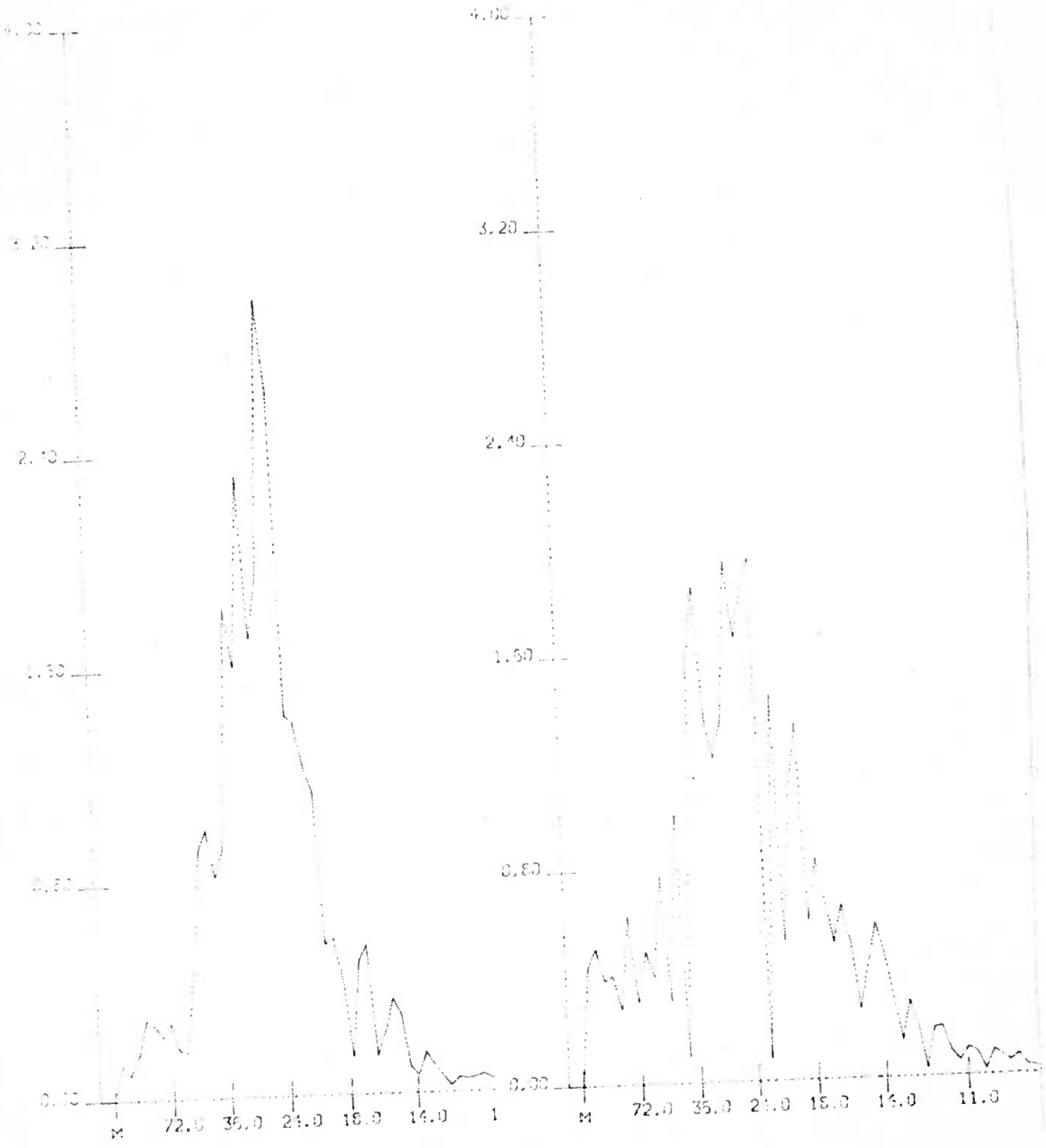


Fig. 4C. MAT: Vertical and N-S Spectral Amplitude ratios, normalized at 42.7 sec., Novaya Zemlya
Start time 7:19:45, Data length 512 sec.


Fig. 4D. CHG: Vertical and N-S Spectral Amplitude ratios, normalized at 42.7 sec, Novaya Zemlya Start time 7:19:45, Data length 512 sec.

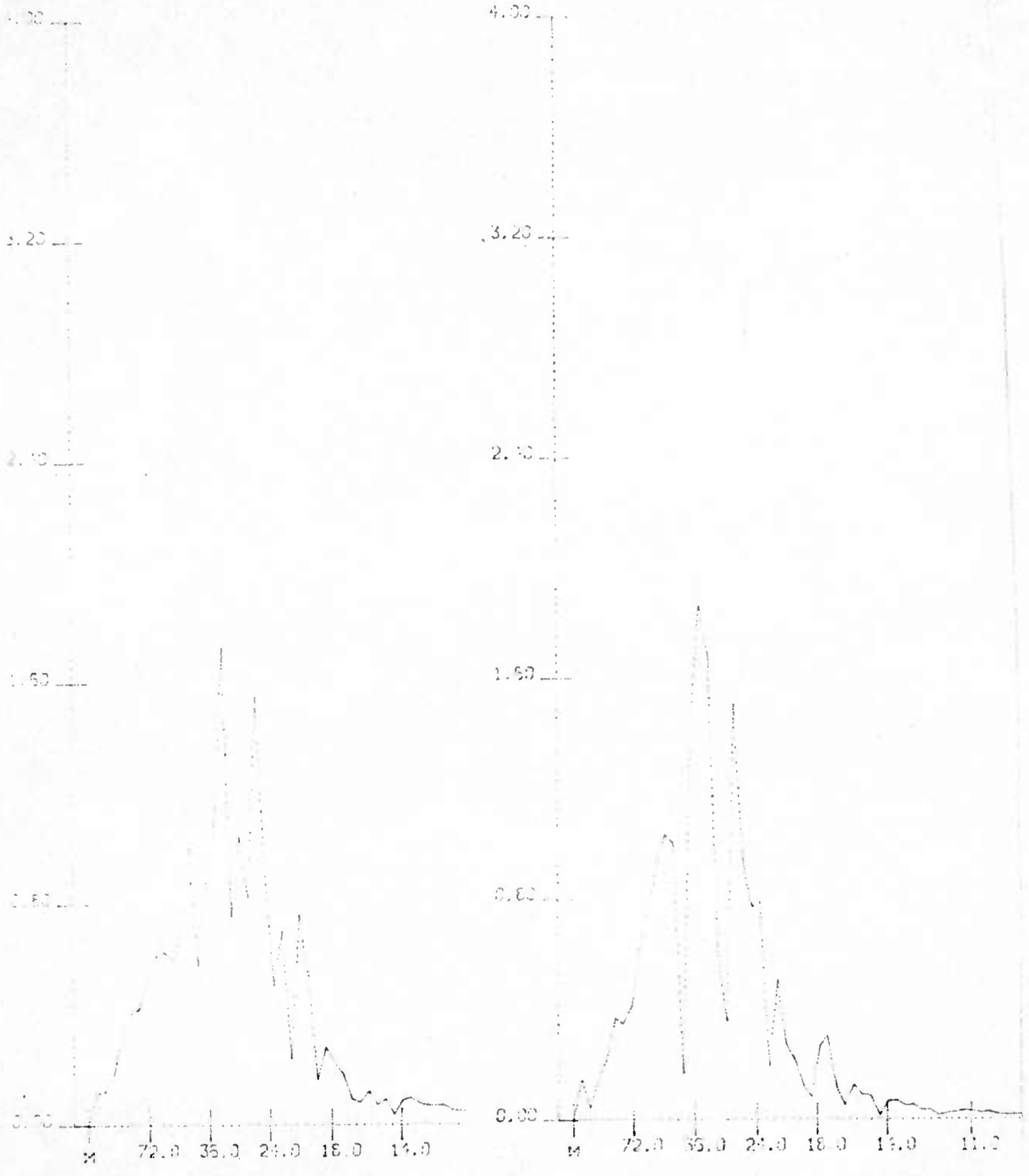


Fig. 4E. ALQ: Vertical and N-S Spectral Amplitude ratios, normalized at 42.7 sec., Novaya Zemlya Start time 7:29:20, Data length 512 sec.

# III

## Papers and Reports Resulting Exclusively from AFOSR Grant 74-2612

### Papers

Eduard Berg: Rayleigh waves from high-gain long-period stations: Signal extraction, amplitude determination, and separation of overlapping wave trains. Bulletin of the Seismological Society of America Vol. 65, No. 6, pp. 1761-1778, December 1975.

Eduard Berg and Duncan M. Chesley: Automated high-precision amplitude and phase calibration of seismic systems. Bulletin of the Seismological Society of America (accepted, to appear probably August 1976).

### Reports

Eduard Berg: Rayleigh waves from high-gain long-period stations: Signal extraction, amplitude determination, and separation of overlapping wave trains, Rept HIG-74-10, Hawaii Institute of Geophysics, Univ. of Hawaii, 29 pp. 21 computer outputs. September 1974.

Duncan M. Chesley and Eduard Berg: Computer programs for seismology: Special applications to the high-gain long-period seismic network. Rept HIG 76-3 Hawaii Institute of Geophysics, Univ. of Hawii, estimated: 75 pages, March 1976.

# IV

# ACKNOWLEDGMENTS

The author wishes to thank graduate assistants Andrew R. Lazarewicz and Duncan M. Chesley who developed the computer software, Jon Peterson and John Hoffman of the Albuquerque Seismological Laboratory who provided the high-gain long-period station digital data, and Dr. G. H. Sutton for helpful discussions and suggestions. Thanks are also expressed to Mr. William J. Best for his continuous interest and support of this work, and Mrs. Ethel McAfee for editing publications and HIG reports.

This research was supported by the Advanced Research Projects Agency of the Department of Defense and was monitored by the Air Force Office of Scientific Research under Contract AFOSR-74-2612.

SECURITY CLASSIFICATION OF THIS PAGE (When Data Entered)

| REPORT DOCUMENTATION PAGE | READ INSTRUCTIONS BEFORE COMPLETING FORM |
|---|---|
| 1. REPORT NUMBER: AFOSR - TR - 76 - 0842 | 2. GOVT ACCESSION NO. |
| 3. RECIPIENT'S CATALOG NUMBER | |
| 4. TITLE (and Subtitle): Rayleigh Waves from High-Gain Long-Period Stations: Signal Extraction, Analytical Determination and Separation of Overlapping Wave Trains; Beam Processing, Calibration of HGLP Stations | 5. TYPE OF REPORT & PERIOD COVERED: Final rept. 1 Oct 1973-31 Mar 1976 |
| | 6. PERFORMING ORG. REPORT NUMBER |
| 7. AUTHOR(s): Eduard Berg | 8. CONTRACT OR GRANT NUMBER(s): AFOSR-74-2612-74; ARPA Order-1827 |
| 9. PERFORMING ORGANIZATION NAME AND ADDRESS: Hawaii Institute of Geophysics, University of Hawaii, Honolulu, Hawaii 96822 | 10. PROGRAM ELEMENT, PROJECT, TASK AREA & WORK UNIT NUMBERS: ARDA Order 1827, Code 4E10 |
| 11. CONTROLLING OFFICE NAME AND ADDRESS: ARPA, 1400 Wilson Boulevard, Arlington, VA 22209 | 12. REPORT DATE: May 1976; 13. NUMBER OF PAGES: 60 |
| 14. MONITORING AGENCY NAME & ADDRESS (if different from Controlling Office): AFOSR/NP, Bolling AFB, Bldg.410, Wash DC 20332 | 15. SECURITY CLASS. (of this report): Unclassified; 15a. DECLASSIFICATION/DOWNGRADING SCHEDULE |

16. DISTRIBUTION STATEMENT (of this Report)

Approved for public release, distributions unlimited.

17. DISTRIBUTION STATEMENT (of the abstract entered in Block 20, if different from Report)

18. SUPPLEMENTARY NOTES

TECH, OTHER

19. KEY WORDS (Continue on reverse side if necessary and identify by block number)

Rayleigh Waves: Detection, amplitude, separation, correlation matched filter, threshold, precision amplitude and phase calibration. Spectral amplitude ratios. Beam forming, computer programs.

20. ABSTRACT (Continue on reverse side if necessary and identify by block number)

For a signal-to-noise ratio between 0.2 and 0.1 on the original single-component records, amplitudes for Rayleigh waves over oceanic paths of 155° at station MAT and 98° at station KIP have been determined as 12 mμ and 24 mμ peak-to-peak, respectively, with a standard error of less than 11 per cent. In each case the processed correlation signal is the highest in a half-hour record. The method makes use of preliminary high-pass filtering and normalized reference earthquake-matched filtering, and takes full advantage of the well-dispersed oceanic surface wave.

The method also provides high resolution of co-located events with short time separation, or of widely spaced events with Rayleigh waves arriving nearly simultaneously at a single station, when the summed vertical and radial matched filtered components are used. Examples include: (1) clear separation and amplitude determination at stations KIP and MAT of two $M_s$ = 6.5 earthquakes located 0.7° and 145 sec apart off the coast of central Chile; (2) clear separation at station KIP of a Novaya Zemlya $m_b$ = 4.8 event from interfering Rayleigh waves of an $m_b$ = 5.0 Kermadec Island earthquake arriving 120 to 140 sec prior to the searched event, with almost complete elimination of interference on the summed vertical and radial processed components; and (3) clear separation at station KIP of two co-located $m_b$ = 4.4 and 4.5 earthquakes 6 min apart off the coast of Chile, with determination of their amplitudes in the presence of interfering Rayleigh waves from two central Alaska earthquakes, the first ($m_b$= 4.1) arriving 15 min prior to the first Chile Rayleigh wave and the second between the two Chile arrivals.

The single-station threshold reached (10 and 25 digital units, p-p) for stations MAT and KIP at 155° and 98°, respectively, corresponds to an $M_s$ = 3.3 and probably can be improved further. Beam focusing is obtained by referring the individual station correlation (reference earthquake matched filter) outputs to the origin time and summing these output from the array of the randomly spaced HGLP stations.

It is shown that the computer determined magnitudes (relative to the reference event) are very stable among different components and different stations and varying by less than 0.1 magnitude.

Automated amplitude and phase response of the complete seismometer-recording system is obtained from step inputs to the calibration coil. High accuracy is achieved by summing as many pulses as desired (to eliminate background noise) by a correlation technique and subsequent Fourier analysis. The only parameters required are the seismometer mass, the Cal-coil constant (referred to the center of mass if appropriate) and current, and the precise onset time of one reference calibration current, which are all very stable over long time periods. Application to the High Gain Long Period system at KIP yields the magnification curve from only six pulses with less scatter ($< \pm 5\%$ for periods larger than 20 sec) than routine steady-state calibrations.

Deconvolution of the digital seismograms results in retrieval of the ground motion (in the frequency range of interest) by the use of the complex Fourier coefficients obtained from the calibration method.

All computer programs developed or used for purpose of this work are presented in a (separate) report.